

A Bayesian Classification Trees Approach to Treatment Effect Variation with Noncompliance

Jared D. Fisher, David W. Puelz, Sameer K. Deshpande

August 16, 2024

Abstract

Estimating varying treatment effects in randomized trials with noncompliance is inherently challenging since variation comes from two separate sources: variation in the impact itself and variation in the compliance rate. In this setting, existing frequentist and flexible machine learning methods are highly sensitive to the weak instruments problem, in which the compliance rate is (locally) close to zero. Bayesian approaches, on the other hand, can naturally account for noncompliance via imputation. We propose a Bayesian machine learning approach that combines the best features of both approaches. Our main methodological contribution is to present a Bayesian Causal Forest model for binary response variables in scenarios with noncompliance by repeatedly imputing individuals' compliance types, allowing us to flexibly estimate varying treatment effects among compliers. Simulation studies demonstrate the usefulness of our approach when compliance and treatment effects are heterogeneous. We apply the method to detect and analyze heterogeneity in the treatment effects in the Illinois Workplace Wellness Study, which not only features heterogeneous and one-sided compliance but also several binary outcomes of interest. We demonstrate the methodology on three outcomes one year after intervention. We confirm a null effect on the presence of a chronic condition, discover meaningful heterogeneity in a "bad health" outcome that cancels out to null in classical partial effect estimates, and find substantial heterogeneity in individuals' perception of management prioritization of health and safety.

1 Introduction

1.1 The effectiveness of workplace wellness programs

Many employers pay their employees to adopt and maintain healthy habits like exercise, diet, or other wellness practices. This pay may be rebates of healthcare premiums and/or compensation in addition to salary. Intuitively, one might expect healthier employees to be more productive and happier in their job. Investing in wellness programs may have additional long-term financial benefits for self-insured employers or those with cost sharing: by promoting healthy behavior, their employees should have better health outcomes in the long-run and incur lower healthcare costs.

To examine the practical effects of workplace wellness programs, a randomized controlled trial was conducted at the University of Illinois at Urbana-Champaign (Jones et al., 2019; Reif et al., 2020). A workplace wellness program, called iThrive, was offered to the treatment group while a control group was also monitored. 12,459 benefits-eligible employees were invited to be part of the study, with 4,834 joining the study. 3,300 of these were assigned to the treatment group and allowed to participate in iThrive. Financial awards were given for participating in the program, though not all invitees actually participated. The other 1,534 subjects were not invited to the program thus comprise the control group. Jones et al. (2019) analyze healthcare spending, job productivity, and health behaviors for 12 and 24 months after the start of the program. They found that subjects with lower medical expenses and healthier habits were more likely to participate in the program once invited; a similar participation discrepancy was found in Mulaney et al. (2021). Jones et al. (2019) analyzed 42 different outcomes and found no significant effect on 40 of them, including medical spending, job productivity, and health behaviors. Participation in iThrive significantly improved the chances that participants received a health screening and believed that their managers prioritized employee health and safety. Reif et al. (2020) extended Jones et al. (2019) for the same cohort by analyzing changes in biometric outcomes and health beliefs. They similarly found that participation in the workplace wellness program had an insignificant effect for most outcomes, including biometrics, diabetes, hypertension, and hospital visits. The only exceptions were that compliant participants (i) were more likely to have a primary care physician and (ii) had more positive beliefs about their own health, on average.

This experiment was not the only study to find that workplace wellness programs may have essentially null results on health outcomes and behaviors. Levy and Thorndike (2019) find that subjects' health outcomes did improve through their 10-week program, but there was no significant difference in healthcare expenses one year after intervention. Song and Baicker (2021) analyze a three-year program, and find that self-reported health behaviors improved, but there was minimal change in health or economic outcomes. However, to quote Mulaney et al. (2021), "One limitation to existing studies is that evidence of health benefits may not have become apparent within the time allowance afforded by these studies." Clearly, studying the effects of workplace wellness programs would be ideal if conducted over decades after the intervention, but long-term studies are uncommon and likely quite expensive, perhaps more than the financial incentives that institutions have for implementing the programs in the first place. There are, however, two statistical phenomena that can help shed further light on the matter. The first is that these trials have noncompliance: subject assigned/invited to the wellness program (the treatment) do not necessarily participate (take the treatment). And second, the treatment effects may be heterogeneous and hard to detect with traditional methods.

1.2 Noncompliance and treatment effect heterogeneity

Randomized controlled trials with noncompliance exists somewhere between observational studies and randomized experiments. The intervention is indeed randomly assigned but is imperfectly taken by the subjects. Two common approaches to deal with noncompliance are instrumental variable techniques and principal stratification. Originally presented by Wright (1928), instrumental variables (IV) provide a way to solve the issue of endogenous treatments. By finding an exogenous variable that is correlated with treatment, but only correlated with the outcome through the treatment, we can estimate the effect of treatment on the outcome,

commonly done through two-stage least squares (Angrist and Pischke, 2009). For trials with noncompliance, the random assignment acts as the instrument — it is only correlated with outcomes through the actual receipt of treatment. Jones et al. (2019) and Song and Baicker (2021) used IV methods to analyze their wellness program studies. Principal stratification refers to identifying different subgroups of interest based on post-randomization variables, such as the actual receipt of treatment in noncompliance. Formalized by Frangakis and Rubin (2002), these subgroups, called principal strata, can have different treatment effects of interest; see Page et al. (2015) for an overview of methods for estimating these subgroup effects.

Treatment effect heterogeneity can also complicate the detection of population treatment effects. It could be the case that some subjects have a positive treatment effect, while other have an opposite, negative treatment effect, resulting in a null population average effect. These two halves of the population likely differ in important ways, and the variables that describe differences in effects are called moderators. When the moderators are not known *a priori*, they must be discovered while estimating the treatment effect heterogeneity. In recent years, tree-based machine learning methods have emerged as popular and effective approaches for this task. Three, in particular, stand out. Hill (2011) proposed a two-step process: first one uses Bayesian additive regression trees (BART; Chipman et al., 2010) to estimate the conditional expectation of the outcome given treatment and covariates; and second, one estimates causal effects with differences in evaluations of the estimated conditional expectation function. Hahn et al. (2020) argued that their Bayesian causal forests (BCF) model, which jointly estimates the prognostic function and treatment effect function with separate BART ensembles, provides more transparent, targeted, and effective regularization of the treatment effects. In contrast with these Bayesian approaches, Wager and Athey (2018) introduced a random forests-based estimator (see also Athey and Wager, 2019).

1.3 Our contributions

We propose a BCF-based approach for to estimate heterogeneous effects of a binary treatment on binary outcomes from randomized trials with one-sided noncompliance. Our work adds to a growing literature on heterogeneous effect estimation with instruments and in the presence of non-compliance. This literature includes Athey et al. (§7 2019) presents a random forests-based IV estimator. Johnson et al. (2022) seeks to detect heterogeneity in the presence of IV, with matching. Using a two-step method, they first find potential effect modifiers with interpretable machine learning method (e.g., a decision tree) and then, second, they test these relationships carefully. McCulloch et al. (2021) and Bargagli-Stoffi et al. (2022) both present BART-based extensions of the popular two-stages least squares approach for IV regression. Chen et al. (2024) jointly model the outcome and the principal strata membership that uses a BCF-style model to predict the outcome and a multinomial BART model to estimate the partially-latent principal strata, which are defined by survival and not treatment compliance. Kim and Zigler (2024) use a similar BCF-based approach to estimate pollution interventions. However, their principal strata are not categorical, as they are defined by a continuous intermediate variable and a binary treatment. Thus, they jointly model the outcome and the intermediate variable instead of the strata membership.

In this paper, we jointly model the binary outcome and compliance status of all subjects in the iThrive study. Across several synthetic datasets, our joint modeling approach type produced more accurate conditional local average treatment effects than methods like GRF and BCF-IV, which use a localized Wald estimator (Wald, 1940), which is a ratio of the conditional intention-to-treat effect on the outcome to that of the treatment receipt.

We find that some of the outcomes from the Illinois Workplace Wellness Study do indeed display treatment effect heterogeneity. One of these is the conditional local average treatment effect of the wellness program on self-report blood measurements: high blood pressure, cholesterol, or glucose. We see that those that treatment compliers who did not report that at least one of these levels was high in 2016 were more likely to self-report in 2017, while those that did self-report in 2016 were not. This suggests that participation in the wellness program made compliant subjects more aware of their own health conditions. We also find the same the significant effect on employees' views about management's health/safety priorities that was found

in Jones et al. (2019), but we also see that different subgroups have varying effect sizes.

This paper proceeds as follows. In Section 2, we carefully define the causal estimand of interest and state the necessary assumptions needed to identify it from the observed data. We then present our estimation strategy in Section 3. We report the results of several simulation studies that compare our proposed approach to existing methods in Section 4. In Section 5, we re-analyze the data from the Illinois workplace wellness study. We conclude in Section 6 with a discussion of the strengths and limitations of our re-analysis and outline several methodological extensions.

2 Identification, heterogeneity, & the pitfalls of IV estimation

For each subject $i = 1, \dots, n$, we observe (i) a p -dimensional covariate vector \mathbf{x}_i ; (ii) a binary indicator A_i recording whether they were invited to participate in the workplace wellness program ($A_i = 1$); (iii) a binary indicator R_i^{obs} recording whether they actually participated in the program ($R_i^{\text{obs}} = 1$) or not ($R_i^{\text{obs}} = 0$); and (iv) a binary outcome $Y_i^{\text{obs}} \in \{0, 1\}$. We ultimately wish to estimate the effect of participating in the workplace wellness program on several binary health outcomes varies with respect to \mathbf{x} . In doing so, we hope to identify who benefits the most from workplace wellness programs and by how much.

Momentarily leaving aside issues of heterogeneity, to determine whether workplace wellness programs have a constant effect on health outcomes, we could naively compare we could naively compare the average responses amongst the treated and control subjects:

$$\frac{\sum_i Y_i^{\text{obs}} \times \mathbb{1}(A_i = 1)}{\sum_i \mathbb{1}(A_i = 1)} - \frac{\sum_i Y_i^{\text{obs}} \times \mathbb{1}(A_i = 0)}{\sum_i \mathbb{1}(A_i = 0)}. \quad (1)$$

Although the comparison is unconfounded due to the random treatment assignment, it can be misleading because not every subject assigned to treatment actually receives treatment. In particular, if the workplace wellness program truly improved health outcomes, then the presence of non-compliers in the treatment arm may deflate the effect estimated by Equation (1). To overcome this bias, it is tempting to compare the average response amongst treated subjects who actually received treatment to the average response amongst the control group:

$$\frac{\sum_i Y_i^{\text{obs}} \times \mathbb{1}(A_i = 1 \ \& \ R_i^{\text{obs}} = 1)}{\sum_i \mathbb{1}(A_i = 1 \ \& \ R_i = 1)} - \frac{\sum_i Y_i^{\text{obs}} \times \mathbb{1}(A_i = 0)}{\sum_i \mathbb{1}(A_i = 0)}. \quad (2)$$

Though intuitive, the estimator in Equation (2) remains unsatisfying in face of non-compliance, as it implicitly assumes that all control subjects would have participated in the wellness program had they been invited. Instead, in principle, ideal comparison is between (i) treated subjects who received treatment and (ii) control subjects who would have received treatment had they been assigned treatment. Unfortunately, we cannot directly carry out the ideal comparison, as it involves reasoning about counterfactual outcome that would have been observed under a potentially different received treatment.

We use potential outcome notation to define precisely the causal quantity of interest, the conditional local average treatment effect. In Section 2.1, we introduce several assumptions under which we can identify LATE in terms of the observed data ($\mathbf{x}_i, A_i, R_i^{\text{obs}}, Y_i^{\text{obs}}$) and present an estimator based on the ratio of two intention-to-treat estimators. Then, in Section 2.2, we turn our attention to the conditional local average treatment effect ($\text{LATE}(\mathbf{x})$) and argue that the natural extension of the ratio estimator can exhibit particularly pathological behavior in the presence of heterogeneous non-compliance.

2.1 Identifying & estimating a constant local average treatment effect

For each subject i , let $R_i(1)$ and $R_i(0)$ denote two potential binary “received treatments” under each treatment assignment. Using the terminology from Angrist et al. (1996), we can stratify our study population into four groups based on the value of $\{R_i(0), R_i(1)\}$: (i) never-takers $\{0, 0\}$; (ii) compliers $\{0, 1\}$; (iii) defiers

$\{1, 0\}$; and (iv) always-takers $\{1, 1\}$. In the workplace wellness study, subjects were not able to participate in the program without an invitation. Thus, for every subject i , we have $R_i(0) = 0$, which implies that there are only never-takers and compliers in our study. We introduce the binary indicator C_i , which encodes whether subject i is a complier ($C_i = 1$) or a never-taker ($C_i = 0$). Note that this means that $C_i = R_i(1)$ and that $R_i(0)$ provides no information about subject i 's compliance status. Finally, for each combination of assigned and potential received treatment $(A_i, R_i(A_i))$, we can define a potential outcome $Y_i(A_i, R_i(A_i))$ to be the outcome observed if a subject was assigned treatment A_i and received treatment $R_i(A_i)$. Each subject in our study has three potential outcomes: (i) the outcome that would be observed if they were invited to participate and did participate in the workplace wellness program $Y_i(1, 1)$; (ii) the outcome if they were invited to participate but ultimately did not participate $Y_i(1, 0)$; and (iii) the outcome if they were not invited to participate $Y_i(0, 0)$. Implicit in our notation is the standard “stable unit treatment value assumption” (SUTVA), which we hereafter denote as Assumption **A1**, that implies that there is no interference across units and that there are no hidden variations of treatment (Imbens and Rubin, 2015). Assumption **A2** encodes our one-sided non-compliance assumption.

A1 (*SUTVA*): Potential outcomes do not vary with treatments assigned to other subjects and, for each subject, there are no different forms or versions of each treatment level, which lead to different treatment outcomes. (Imbens and Rubin, 2015).

A2 (*One-sided Noncompliance*): for all subjects i , $R_i(0) = 0$.

Our assumption of one-sided non-compliance (Assumption **A2**) is stronger than the “no defiers”/monotonicity assumption that is traditionally assumed many principal stratification settings (e.g. Imbens and Rubin, 2015, Section 24.5.2) as it also does not allow for always-takers. It is, however, a very reasonable assumption in many circumstances where subjects have no path to receive the treatment except through invitation. Armed with this notation, we can define the (constant) local average treatment effect

$$\text{LATE} = \mathbb{E}[Y_i(1, 1) - Y_i(0, 0) | C_i = 1]. \quad (3)$$

In order to identify the constant LATE, we make several assumptions, many of which are standard, and apply for all for all subjects i .

A3 (*Exclusion Restriction*): Assignment to treatment has no effect on the outcome except through the receipt of treatment: $Y_i(0, 0) = Y_i(1, 0)$.

A4 (*Unconfoundedness*) Potential outcomes and received treatments are independent of assigned treatment: $A_i \perp [R_i(0), R_i(1), Y_i(0, 0), Y_i(1, 0), Y_i(1, 1)]$

A5 (*Existence of Compliers*): $0 < \mathbb{P}(C_i = 1)$

A6 (*Overlap*): $0 < \mathbb{P}(A_i = 1) < 1$

Assumption **A3** encodes the belief that assignment to treatment affects the outcome only through the actual receipt of treatment. Assumption **A4** is usually satisfied by random treatment assignment. Assumptions **A5** and **A6** allow estimation to be meaningful, as there are at least some compliers and some units assigned to each treatment arm.

Under Assumptions **A1–A6**, we could identify LATE as

$$\text{LATE} = \mathbb{E}[Y_i^{\text{obs}} | C_i = 1, A_i = 1] - \mathbb{E}[Y_i^{\text{obs}} | C_i = 1, A_i = 0] \quad (4)$$

if we could observe the compliance status of all subjects. Equation (4) suggests a very natural estimator: we simply compare the average outcomes amongst compliers in each treatment arm. Unfortunately, we only observe $\mathbf{C}^{(1)} = \{C_i : A_i = 1\}$ and do not observe $\mathbf{C}^{(0)} = \{C_i : A_i = 0\}$.

To overcome this difficulty, it is common in the instrumental variables literature to estimate LATE with the Wald estimator (Wald, 1940), defined as the ratio of two “intention-to-treat” (ITT) estimates. To motivate

such estimators, first observe that under Assumptions [A1](#) and [A4](#) (see [Appendix B](#)), we can identify the ITT_Y :

$$\text{ITT}_Y := \mathbb{E}[Y_i(1, R_i(1)) - Y_i(0, R_i(0))] = \mathbb{E}[Y_i^{\text{obs}} | A_i = 1] - \mathbb{E}[Y_i^{\text{obs}} | A_i = 0]. \quad (5)$$

We can similarly define the ITT_R :

$$\text{ITT}_R := \mathbb{E}[R_i(1) - R_i(0)] = \mathbb{E}[R_i^{\text{obs}} | A_i = 1] - \mathbb{E}[R_i^{\text{obs}} | A_i = 0]. \quad (6)$$

Assumptions [A1-A3](#) and [A5](#) allow us to write $\text{LATE} = \text{ITT}_Y / \text{ITT}_R$, which provides the same estimator as a two-stage least squares IV regression with no covariates ([Angrist and Pischke, 2009](#), Section 4.1.2). Combining these ideas, we get that

$$\text{LATE} = \frac{\mathbb{E}[Y_i^{\text{obs}} | A_i = 1] - \mathbb{E}[Y_i^{\text{obs}} | A_i = 0]}{\mathbb{E}[R_i^{\text{obs}} | A_i = 1] - \mathbb{E}[R_i^{\text{obs}} | A_i = 0]} = \frac{\mathbb{P}(Y_i^{\text{obs}} = 1 | A_i = 1) - \mathbb{P}(Y_i^{\text{obs}} = 1 | A_i = 0)}{\mathbb{P}(R_i^{\text{obs}} = 1 | A_i = 1)}. \quad (7)$$

where the second equality follows from [Assumption A2](#) and the fact that Y_i^{obs} and R_i^{obs} are binary.

2.2 The *conditional* local average treatment effect

Up to this point, our discussion has focused on estimating a constant effect. In reality, we believe it more likely that the workplace wellness program will benefit only some subjects but not others. Further, we believe that not all subjects are equally likely to be compliers. To probe potential heterogeneity, we focus on a natural analog of LATE, the *conditional* local average treatment effect

$$\text{LATE}(\mathbf{x}) = \mathbb{E}[Y_i(1, 1) - Y_i(0, 0) | C_i = 1, \mathbf{X}_i = \mathbf{x}]. \quad (8)$$

To identify $\text{LATE}(\mathbf{x})$, we replace [Assumption A4-A6](#) with their stronger, *conditional* versions.

Ax4 (Unconfoundedness): The potential outcomes and received treatments are conditionally independent of assigned treatment given \mathbf{x} : $A_i \perp [R_i(0), R_i(1), Y_i(0, 0), Y_i(1, 0), Y_i(1, 1)] | \mathbf{X}_i = \mathbf{x}$.

Ax5 (Existence of Compliers): $0 < \mathbb{P}(C_i = 1 | \mathbf{X}_i = \mathbf{x})$

Ax6 (Overlap): $0 < \mathbb{P}(A_i = 1 | \mathbf{X}_i = \mathbf{x}) < 1$

Under these assumptions, we would ideally estimate

$$\text{LATE}(\mathbf{x}) = \mathbb{E}[Y_i^{\text{obs}} | C_i = 1, A_i = 1, \mathbf{X}_i = \mathbf{x}] - \mathbb{E}[Y_i^{\text{obs}} | C_i = 1, A_i = 0, \mathbf{X}_i = \mathbf{x}]. \quad (9)$$

Because we do not fully observe \mathbf{C} , we cannot operationalize Equation (9), by, for instance, regressing Y_i^{obs} onto A_i and \mathbf{X}_i using data from the compliers. Under [Assumptions A1-A3](#) and [Assumptions Ax4-Ax6](#), a natural extension of the ratio estimator in Equation (7) is

$$\text{LATE}(\mathbf{x}) = \frac{\mathbb{P}(Y_i^{\text{obs}} = 1 | A_i = 1, \mathbf{X}_i = \mathbf{x}) - \mathbb{P}(Y_i^{\text{obs}} = 1 | A_i = 0, \mathbf{X}_i = \mathbf{x})}{\mathbb{P}(R_i^{\text{obs}} = 1 | \mathbf{X}_i = \mathbf{x})} \quad (10)$$

There are many ways to implement an estimator in Equation (10) by separately modeling the numerator and denominator. To estimate the numerator, we could use the ‘‘TS-learner’’ framework of [Künzel et al. \(2019\)](#) and separately regress the outcome Y^{obs} onto the covariates \mathbf{X} in each treatment arm. Alternatively, we could follow their ‘‘S-learning’’ framework and fit a single regression model that predicts Y^{obs} using both the covariates \mathbf{X} and the assigned treatment A . Regardless of how we estimate the numerator, however, the estimator in Equation (10) becomes extremely unstable whenever $\mathbb{P}(R_i^{\text{obs}} = 1 | A_i = 1, \mathbf{X}_i = \mathbf{x})$ is near zero. So, estimating $\text{LATE}(\mathbf{x})$ for individuals who are unlikely to comply with the assigned treatment can be fraught. This situation is termed the ‘‘weak instrument problem.’’

2.3 The weak instrument problem and the local compliance rate

In the instrumental variables analyses, an important consideration is the relevance of the instrument, i.e. the strength of the instrument’s relationship with the treatment. For us, the instrument is the assignment to treatment A_i and the treatment is $R_i(A_i)$. If A_i has no causal effect on $R_i(A_i)$, then clearly $ITT_R = \mathbb{E}[R_i(1) - R_i(0)] = 0$ and the Wald estimator is undefined. Under the aforementioned assumptions, as $R_i(1) = C_i$ and $R_i(0) = 0$, we see that this denominator is equivalent to the compliance rate $\mathbb{P}(C_i = 1)$.

The weak instrument problem is well known (Andrews et al., 2019), and a compliance rate near zero would be an obvious indicator of a challenged experiment. However, as we move from estimating global LATE to conditional LATE, and specifically move from Assumption A5 to Assumption Ax5, we have another consideration: heterogeneity in compliance rate may mean that, while the global compliance rate is reasonable, the compliance rate local certain values of \mathbf{X} may present a locally weak instrument. In Section 3, we propose an alternative that does not use the standard Wald estimator but instead models compliance, akin to Ratkovic and Shiraito (2014) and Imbens and Rubin (2015). Later we examine, via simulation, what happens when heterogeneous compliance rates yield locally weak instruments in Section 4.1.

3 Estimating LATE with BART

We essentially must estimate the response surface $\mathbb{P}(Y_i^{\text{obs}} = 1 | C_i = c, A_i = a, \mathbf{X}_i = \mathbf{x})$ without observing \mathbf{C} , the full set of compliance statuses. To this end, we specify a joint model for $(Y^{\text{obs}}, \mathbf{C})$ that will allow us to (i) impute the missing compliance statuses $\mathbf{C}^{(0)}$ and then (ii) conditionally estimate the needed response surface. Specifically, we model

$$\begin{aligned} \mathbb{P}(Y_i = 1 | C_i = c_i, A_i = a_i, \mathbf{X}_i = \mathbf{x}_i) &= \Phi(\mu(\mathbf{x}_i) + c_i \times \mu_c(\mathbf{x}_i) + c_i \times a_i \times \tau(\mathbf{x}_i)) \\ \mathbb{P}(C_i = 1 | \mathbf{X}_i = \mathbf{x}_i) &= \Phi(\eta(\mathbf{x}_i)). \end{aligned} \tag{11}$$

We approximate each of μ , μ_c , τ , and η with a regression tree ensemble and computing a joint posterior distribution over the missing compliance statuses and the tree ensembles. Since the posterior distribution is analytically intractable, we simulate draws from the posterior over regression tree ensembles using Markov chain Monte Carlo.

3.1 Prior regularization

Before specifying the prior and describing our posterior sampling strategy, we assume without loss of generality that all continuous covariates are re-scaled to the interval $[0,1]$ and introduce some additional notation. A regression tree (T, \mathcal{B}) is comprised of a binary decision tree T , which consists of collection of internal nodes and a collection of terminal or leaf nodes, and a collection \mathcal{B} of scalar jumps, one for each leaf. Each internal node of T is associated with a decision rule $\{X_j \in \mathcal{C}\}$. When X_j is continuous variable, \mathcal{C} is a half-open interval of the form $[0, c)$ and when X_j is categorical, \mathcal{C} is a subset of the possible levels of that variable. Given T , we can associate each \mathbf{x} with a single leaf by tracing a path down the tree by following the decision rules. Specifically, whenever the path encounters the rule $\{X_j \in \mathcal{C}\}$, it proceeds to the left (resp. right) if $x_j \in \mathcal{C}$ (resp. $x_j \notin \mathcal{C}$). This way, the decision tree T partitions the covariate space into disjoint regions, one for each leaf. Denoting the jump associated with leaf ℓ as β_ℓ , the pair (T, \mathcal{B}) , represents a piece-wise constant function that returns β_ℓ for all \mathbf{x} in the region associated with leaf ℓ . Figure 1 shows an example of a regression tree.

For compactness, we use $\mathcal{E}^{(\mu)} = \{(T_m^\mu, \mathcal{B}_m^\mu) : m = 1, \dots, M^{(\mu)}\}$ to denote the ensemble of $M^{(\mu)}$ regression trees used to approximate μ . We similarly define $\mathcal{E}^{(\mu_c)}$, $\mathcal{E}^{(\tau)}$, and $\mathcal{E}^{(\eta)}$ for the remaining ensembles. Like Hahn et al. (2020) and Deshpande et al. (2024), we specify independent priors for each ensemble in \mathcal{E} and place independent and identical priors on the regression trees within each ensemble.

For ease of exposition, we only describe the regression tree prior for $\mathcal{E}^{(\mu)}$ as the priors for the remaining ensembles are analogous. The regression tree prior consists of three parts: (i) a marginal prior over the

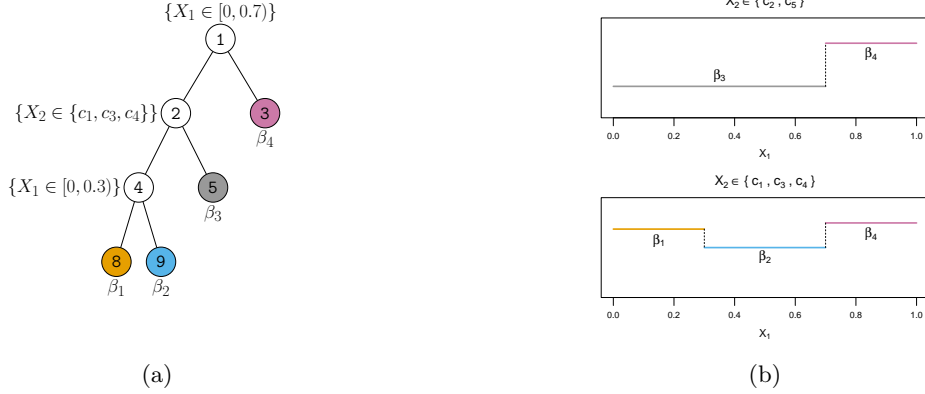


Figure 1: A regression tree defined over $\mathcal{X} = [0, 1] \times \{c_1, \dots, c_5\}$ (a) and its step function representation (b).

structure of the decision tree; (ii) a conditional prior over the decision rules given the tree structure; and (iii) a condition prior for the jumps \mathcal{B} given the decision tree.

We can describe the tree structure prior with a branching process in which nodes are added sequentially so that whenever a new node is added at depth d , two children at depth $d+1$ are attached to it with probability $0.95(1+d)^{-2}$. This prior places overwhelming prior probability on trees of depth five or less.

Conditional on the tree structure, we sequentially draw decision rules at each non-terminal node in two steps. First, we draw the splitting variable index $j \sim \text{Multinomial}(\theta_1^{(\mu)}, \dots, \theta_p^{(\mu)})$. Then, conditional on j , we set \mathcal{C} to be a random subset of $\mathcal{A}(j)$, the set of available X_j values at the current non-terminal node. If X_j is continuous, we set $\mathcal{C} = [0, c)$ where c is drawn uniformly from the interval $\mathcal{A}(j)$. Otherwise, if X_j is categorical, we set \mathcal{C} to be a random non-trivial subset of the discrete set $\mathcal{A}(j)$. In Figure 1, at the node labelled 8, we have $\mathcal{A}(1) = [0, 0.3)$ and $\mathcal{A}(2) = \{c_1, c_3, c_4\}$. Following Linero (2018), we model $(\theta_1^{(\mu)}, \dots, \theta_p^{(\mu)}) \sim \text{Dirichlet}(\xi^{(\mu)}/p, \dots, \xi^{(\mu)}/p)$ and $\xi^{(\mu)}/(\xi^{(\mu)} + p) \sim \text{Beta}(0.5, 1)$.

Finally, conditional on the decision tree T , we respectively place independent $\mathcal{N}(\beta_0^{(\mu)}/M^{(\mu)}, \sigma^{2(\mu)}/M^{(\mu)})$ on the jumps in \mathcal{B} , where $\beta_0^{(\mu)}$ and $\sigma^{(\mu)}$ are fixed constants. We specify similar priors for the other ensembles $\mathcal{E}^{(\mu_c)}$, $\mathcal{E}^{(\tau)}$, and $\mathcal{E}^{(\eta)}$. We recommend using 50 trees in each ensemble (i.e., setting $M^{(\mu)} = M^{(\mu_c)} = M^{(\tau)} = M^{(\eta)} = 50$) and the following hyper-parameter settings: $(\beta_0^{(\mu)}, \sigma^{(\mu)}) = (\Phi^{-1}(\bar{y}), 1.5)$; $(\beta_0^{(\eta)}, \sigma^{(\eta)}) = (\Phi^{-1}(\bar{c}), 1.5)$; $(\beta_0^{(\mu_c)}, \sigma^{(\mu_c)}) = (0, 0.5)$; and $(\beta_0^{(\tau)}, \sigma^{(\tau)}) = (0, 0.5)$ where \bar{y} is the average response in the whole dataset and \bar{c} is the observed compliance rate among treated subjects. These choices imply the following marginal priors: $\mu(\mathbf{x}) \sim \mathcal{N}(\Phi^{-1}(\bar{y}), 1.5^2)$; $\eta(\mathbf{x}) \sim \mathcal{N}(\Phi^{-1}(\bar{c}), 1.5^2)$; $\mu_c(\mathbf{x}) \sim \mathcal{N}(0, 0.5^2)$; and $\tau(\mathbf{x}) \sim \mathcal{N}(0, 0.5^2)$. In other words, we shrink each subjects' compliance and outcome probabilities towards the overall averages observed in the dataset. Bounding the conditional LATE with the first-order approximation

$$\text{LATE}(\mathbf{x}) \approx \tau(\mathbf{x}) \times \phi(\mu(\mathbf{x}) + c \times \mu_c(\mathbf{x})) \leq (2\pi)^{-1/2} |\tau(\mathbf{x})|,$$

our prior places approximate 68% probability on the event that $|\text{LATE}(\mathbf{x})| < 0.2$. In the context of the workplace wellness studies, a 20-percentage point effect is quite large, making our prior on $\text{LATE}(\mathbf{x})$ fairly weakly informative.

3.2 Posterior computation

We use a Gibbs sampler to simulate draws from the joint posterior distribution $p(\mathcal{C}^{(0)}, \mathcal{E}, \Theta, \xi, \mathbf{Y}, \mathcal{C}^{(1)})$, where $\Theta = \{\theta^{(\mu)}, \theta^{(\mu_c)}, \theta^{(\tau)}, \theta^{(\eta)}\}$ is the collection of prior splitting probabilities for each ensemble and $\xi = \{\xi^{(\mu)}, \xi^{(\mu_c)}, \xi^{(\tau)}, \xi^{(\eta)}\}$ are the corresponding prior hyperparameters. We provide a high-level overview

of the sampler here and present a detailed derivation in Appendix A. Each iteration of our sampler involves four steps. In the first step, we draw the missing compliance statuses $\mathbf{C}^{(0)}$ conditionally given the ensembles \mathcal{E} and \mathbf{Y} . Under (11), it turns out that the missing compliance statuses are conditionally independent of one another given \mathcal{E} and \mathbf{Y} (see Equations (A13) and (A14) in Appendix A.1).

After drawing the missing $\mathbf{C}^{(0)}$, we sequentially update each regression tree in \mathcal{E} in the second step of our sampler. To facilitate these updates, we introduce latent utilities \tilde{Y}_i and \tilde{C}_i such that $Y_i = \mathbb{1}(\tilde{Y}_i \geq 0)$ and $C_i = \mathbb{1}(\tilde{C}_i)$. Conditional on these latent utilities, we sweep over the trees in \mathcal{E} , updating them one at a time while holding the others fixed. Each individual tree update proceeds in two steps. First, we draw a new tree structure from its *marginal* distribution using a Metropolis-Hastings step in which proposals are drawn by randomly growing or pruning the current tree structure. Then, we draw a new collection of jumps \mathcal{B} from its conditional distribution given the new tree structure and all other regression trees. Essentially, these tree updates turn out to be nothing more than a weighted version of Chipman et al. (2010)’s original Bayesian backfitting strategy that was also used in Hahn et al. (2020) and Deshpande et al. (2024).

Once we have updated each regression tree in \mathcal{E} , we sample new values of each vector in Θ conditionally on $\boldsymbol{\eta}$ using a conjugate Dirichlet-Multinomial update before drawing new values of $\boldsymbol{\eta}$ using an independence Metropolis step.

4 Simulations

We investigated the operating characteristics of our proposed approach (hereafter BCF-LATE) using three synthetic data simulation studies. We compared BCF-LATE with two versions of the Wald estimator (Equation (10)): GRF, the generalized random forest of Athey et al. (2019), and Wald-BART, which uses BART to estimate the expectations in the numerator and denominator of the Wald estimator. We specifically assessed how well each method could (i) predict evaluations $\text{LATE}(\mathbf{x})$ out-of-sample and (ii) quantify its uncertainty about those predictions. For each study, we generated n observations $(\mathbf{x}_1, A_1, R_1^{\text{obs}}, Y_1^{\text{obs}}), \dots, (\mathbf{x}_n, A_n, R_n^{\text{obs}}, Y_n^{\text{obs}})$ as follows. First, we drew the covariates $\mathbf{x}_i \in [-1, 1]^p$ uniformly. Then we drew the random treatment assignment A_i , treatment receipt R_i^{obs} , and outcome Y_i^{obs} as

$$\begin{aligned} a_i &\sim \text{Bernoulli}(0.5) & c_i &\sim \text{Bernoulli}(p_i^c) & p_i^c &= \Phi[\eta(\mathbf{x}_i)] \\ r_i &= a_i c_i & y_i &\sim \text{Bernoulli}(p_i^y) & p_i^y &= \Phi[\mu(\mathbf{x}_i) + c_i \mu_c(\mathbf{x}_i) + a_i c_i \tau(\mathbf{x}_i)]. \end{aligned}$$

We used different functions μ , μ_c , τ , and η in each simulation study.

4.1 Illustrating the weak instrument problem with a single covariate

To visualize the differences between each method, we set $p = 1$ for our first simulation study. For this study, we drew each \mathbf{x}_i uniformly from $[-1, 1]$ and generated the data using

$$\eta(x) = 0 \quad \mu(x) = \sin(6x) \quad \mu_c(x) = -x \quad \tau(x) = 2 \times \mathbb{1}(x \leq 0) - 1$$

The top row of Figure 2 shows each of $\mu(x)$, $\mu_c(x)$ and $\tau(x)$ with BCF-LATE’s posterior mean (solid line) and 50%, 80%, and 95% pointwise posterior credible intervals (shaded regions) overlaid in blue. BCF-LATE recovers each of $\mu(x)$, $\mu_c(x)$, and $\tau(x)$ reasonably well; the 95% pointwise credible intervals for $\mu(x)$ and $\mu_c(x)$ had more than the nominal 95% frequentist coverage and the intervals for $\tau(x)$ covered about 88% of evaluations on average across 100 replications. Although $\tau(x)$ takes only two values, the function of interest, $\text{LATE}(x)$ is more complicated (bottom row of Figure 2). In this setting with a moderate, homogeneous compliance rate, all three methods performed similarly, with BCF-LATE enjoying a slight advantage. Across 100 simulation replications, the average root mean square errors (RMSE) for evaluating $\text{LATE}(x)$ were 0.105 (BCF-LATE), 0.110 (Wald-BART), and 0.114 (GRF) and the average coverage of the 95% uncertainty intervals were 86.9% (BCF-LATE), 97.4% (Wald-BART), and 86.1% (GRF). While Wald-BART’s coverage is much closer

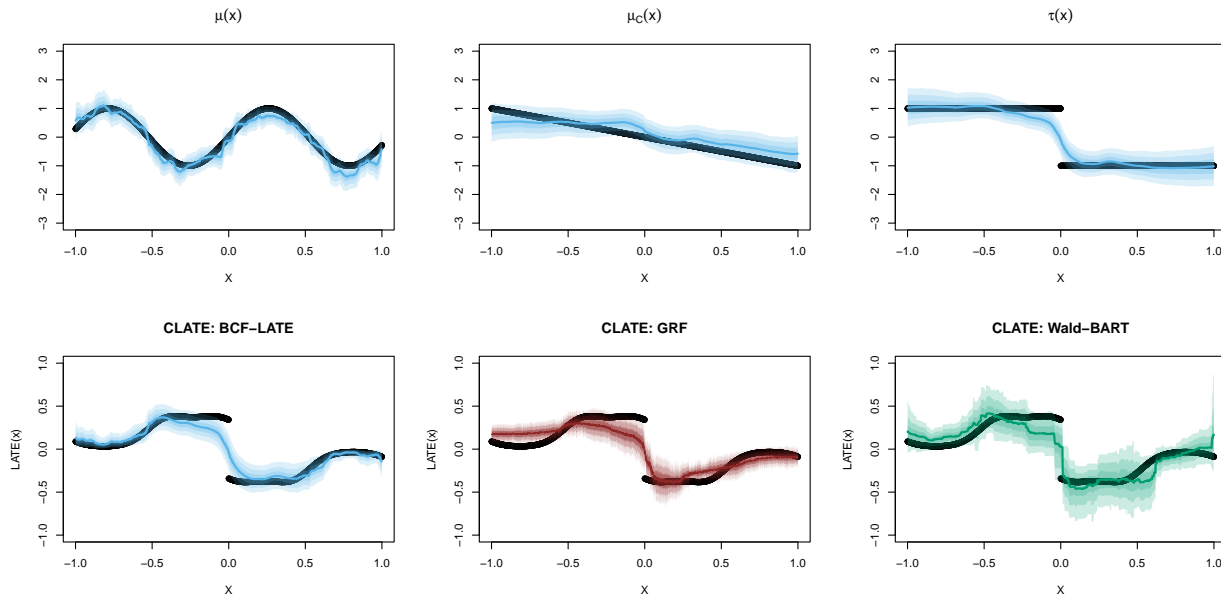


Figure 2: Comparison of different methods’ estimation of heterogeneous CLATEs when a univariate data-generating process has a constant, large compliance rate. For BCF-LATE and Wald-BART, we shade the pointwise 50%, 80%, and 95% credible intervals. For GRF the shaded region shows the mean plus/minus 0.65, 1.3, and 2 standard errors.

to the target 95%, we note that its intervals are much wider than the other methods, as is visible in the bottom row of panes in Figure 2.

While it is reassuring that BCF-LATE performs well when all subjects have the same, moderately large compliance probability, the heterogeneous compliance setting is arguably more relevant. Recall from Section 2, that we observe three types of subjects, each with their own outcome model:

$$\mathbb{P}(Y_i = 1|C_i, A_i, \mathbf{X}_i = \mathbf{x}) = \begin{cases} \Phi[\mu(\mathbf{x})] & \text{if } C_i = 0 \\ \Phi[\mu(\mathbf{x}) + \mu_c(\mathbf{x})] & \text{if } C_i = 1 \text{ and } A_i = 0 \\ \Phi[\mu(\mathbf{x}) + \mu_c(\mathbf{x}) + \tau(\mathbf{x})] & \text{if } C_i = 1 \text{ and } A_i = 1 \end{cases} \quad (12)$$

Intuitively, we might expect to estimate $\mu(x)$ well when there is a large number of never-takers with $x_i \approx x$. Similarly, because there is no uncertainty about compliance status in the treatment arm, we would expect to estimate $\mu(x) + \mu_c(x) + \tau(x)$ well whenever there is a large number of invited compliers with $x_i \approx x$. So, if there are reasonably large sets of never-takers and invited compliers with $x_i \approx x$ we would expect BCF-LATE to estimate the difference $\mu_c(x) + \tau(x)$ well. To estimate $\text{LATE}(x)$, however, we must disentangle $\mu_c(x)$ from $\tau(x)$. This is best done when the compliance rate when $\mathbb{P}(C_i = 1|x_i = x)$ is not too small and there are large numbers of compliers with $x_i \approx x$.

To check this intuition, we re-ran the simulation study using the same data generating functions $\mu(x)$ and $\mu_c(x)$ as before but this time with $\eta(x) = -2x$. Figure 3 shows how BCF-LATE recovers each of $\mu(x)$, $\mu_c(x)$, $\tau(x)$, $\mathbb{P}(C = 1|x)$, $\mu_c(x) + \tau(x)$, and $\text{LATE}(x)$.

As anticipated, when x is small and the compliance rate is close to one (yielding few never-takers), the uncertainty bands of $\mu(x)$ widen in the top left pane. However, when there is a reasonable local sample size of never-takers (i.e., when the compliance rate is not close to 1), the function is well-estimated and the uncertainty intervals are tighter. Similarly, for values of more central values of x yielding non-extreme

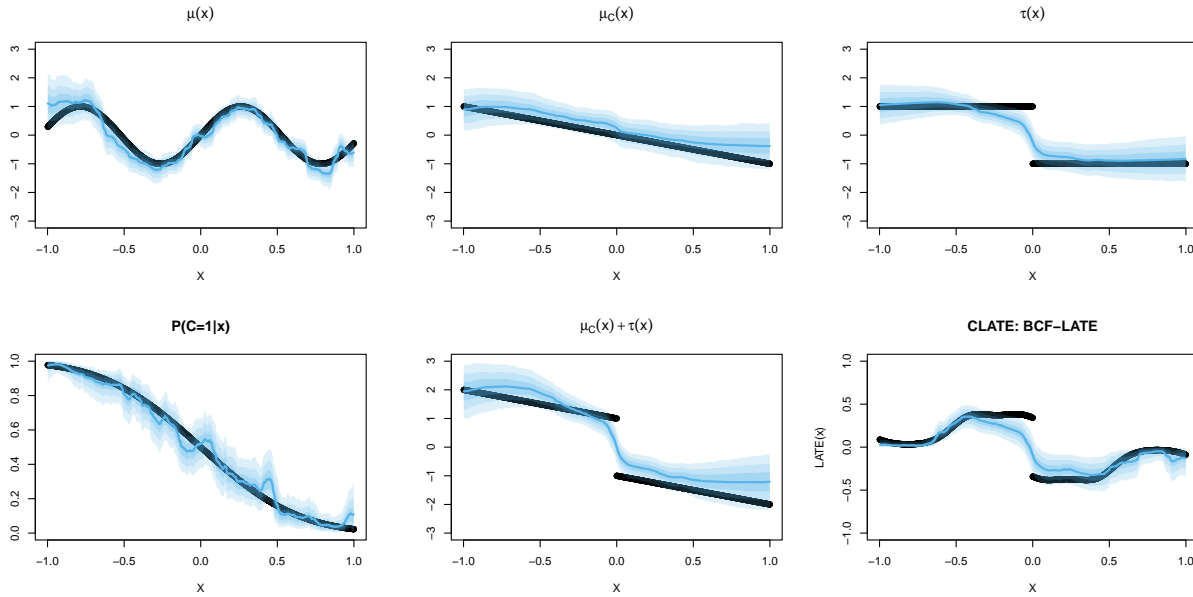


Figure 3: BCF-LATE fits for a univariate data-generating process with heterogeneous outcome and heterogeneous compliance. We shade the pointwise 50%, 80%, and 95% credible intervals.

compliance probabilities, BCF-LATE produced shorter uncertainty intervals for $\mu_c(x) + \tau(x)$. For values of x closer to ± 1 , which produce extreme compliance probabilities, BCF-LATE returned much more uncertainty about this function. Turning to $LATE(x)$, we find that BCF-LATE produced accurate estimates and well-calibrated uncertainty intervals.

Figure 4 compares BCF-LATE’s ability to estimate $LATE(x)$ in the presence of a weakening instrument with those of GRF and Wald-BART. As expected, all three methods do well when the compliance rate is large. However, as x increases and the compliance probability drops, we see that the uncertainty intervals for GRF and Wald-BART become much more erratic and inflated. Visually it further appears that BCFLATE produced more accurate estimates of $LATE(x)$, especially when the compliance probability was low. In fact, across 100 simulation replications, BCFLATE’s average RMSE was 0.114, which was smaller than GRF’s (0.289) and Wald-BART’s (0.883).

4.2 Multiple covariates

Our second simulation study assessed how well BCF-LATE performs when n and p increase but when the underlying data-generating functions are relatively simple. For this study, for each combination of $n \in \{500, 2000, 5000\}$ and $p \in \{2, 5, 10, 25, 50, 75, 100\}$, we generated 100 datasets of size n using the functions

$$\eta(\mathbf{x}) = 4 \times \mathbb{1}(x_2 \geq 0.5) - 2 \quad \mu(\mathbf{x}) = \mu_c(\mathbf{x}) = 0 \quad \tau(\mathbf{x}) = 4 \times \mathbb{1}(x_1 \geq 0.5) - 2.$$

Figure 5 shows GRF’s RMSE (left) and interval score (right) relative to BCF-LATE’s as a function of p with $n = 2000$ fixed. The interval score combines interval coverage and interval width and is a proper scoring rule (Gneiting and Raftery, 2007). In the figure, values greater (resp. less) than one indicate that BCF-LATE performs better (resp. worse) than GRF. We see that for $n = 2000$ and small p , BCF-LATE is markedly better than GRF at estimating $LATE(x)$. While this performance gap shrinks as p increases, it does not go away: for $p = 5$, BCF-LATE’s RMSE is four times smaller than GRF’s and for $p = 100$, it is two times smaller. On further inspection, we found that as p increased, the width and coverage of BCF-LATE’s intervals increased while the width and coverage of GRF’s intervals decreased; see Table C3.

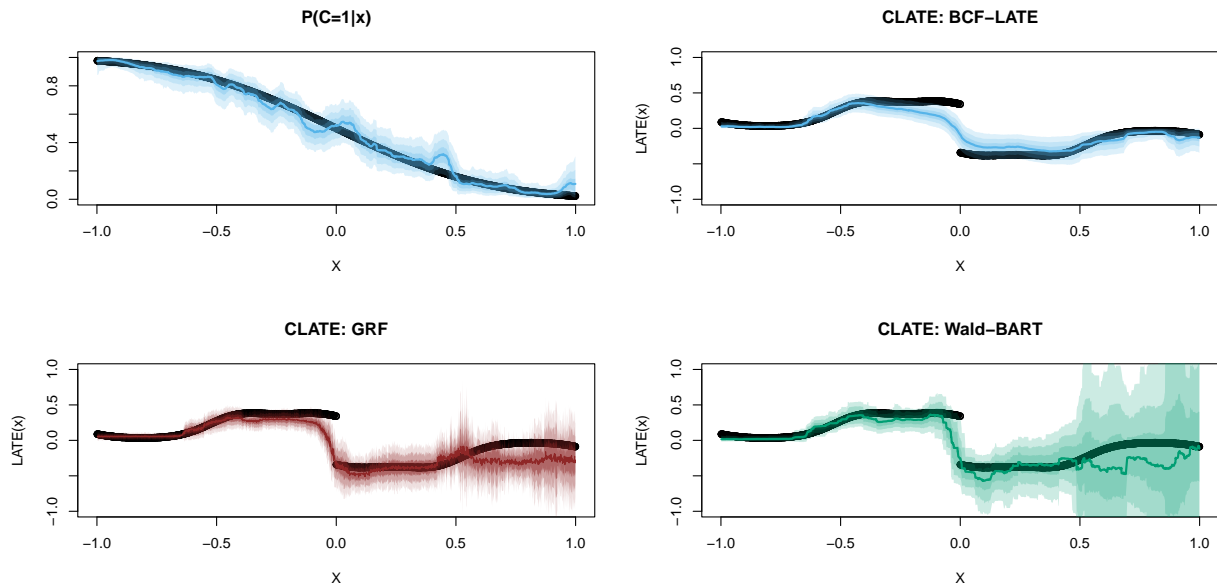


Figure 4: Comparison of different methods’ estimation of heterogeneous CLATEs from a univariate data-generating process. The compliance rate varies such that the instrument is weak when x is large. For BCF-LATE and Wald-BART, we shade the pointwise 50%, 80%, and 95% credible intervals. For GRF the shaded region shows the mean plus/minus 0.65, 1.3, and 2 standard errors.

Figure 6 is analogous to Figure 5 and shows how GRF’s relative RMSE and interval score changes as n increases while fixing $p = 25$. BCF-LATE’s edge in performance grows with the sample size n , for both point and interval estimation; see Table C4 for tabulation of these results.

4.3 Complicated Data Generating Process

In our third simulation study, we generated data with somewhat more complicated functions:

$$\begin{aligned}
 \tau(x) &= \sin(\pi x_1 x_2) - (x_3 - 0.5)^2 + .1x_4 - .2x_5 \\
 \eta(x) &= \exp(x_3) - x_1 - x_2 - x_4 - x_5 \\
 \mu(x) &= 2 \times \mathbb{1}(x_2 + x_5 > 1) - x_3 \\
 \mu_C(x) &= x_1 x_3 - x_4
 \end{aligned}$$

For each combination of $n \in \{500, 2000, 5000\}$ and $p \in \{5, 10, 25, 50, 75, 100\}$, we generated 100 synthetic datasets of size n . Figures 7 and 8 are analogs of Figures 5 and 6, comparing the performance of GRF to BCF-LATE as p and n increase. Like before, we find that the gap between GRF and BCF-LATE diminishes as p increases while keeping n fixed and the gap increases somewhat as n increases while keeping p fixed; see Tables C5 and C6 for more details. Across nearly all combinations of n and p , BCF-LATE had smaller RMSE and interval score than GRF.

We conclude from our simulation studies that BCF-LATE is at least as capable as — and often better than — GRF in estimating the conditional local average treatment effects $LATE(x)$ in terms of point and interval estimation.

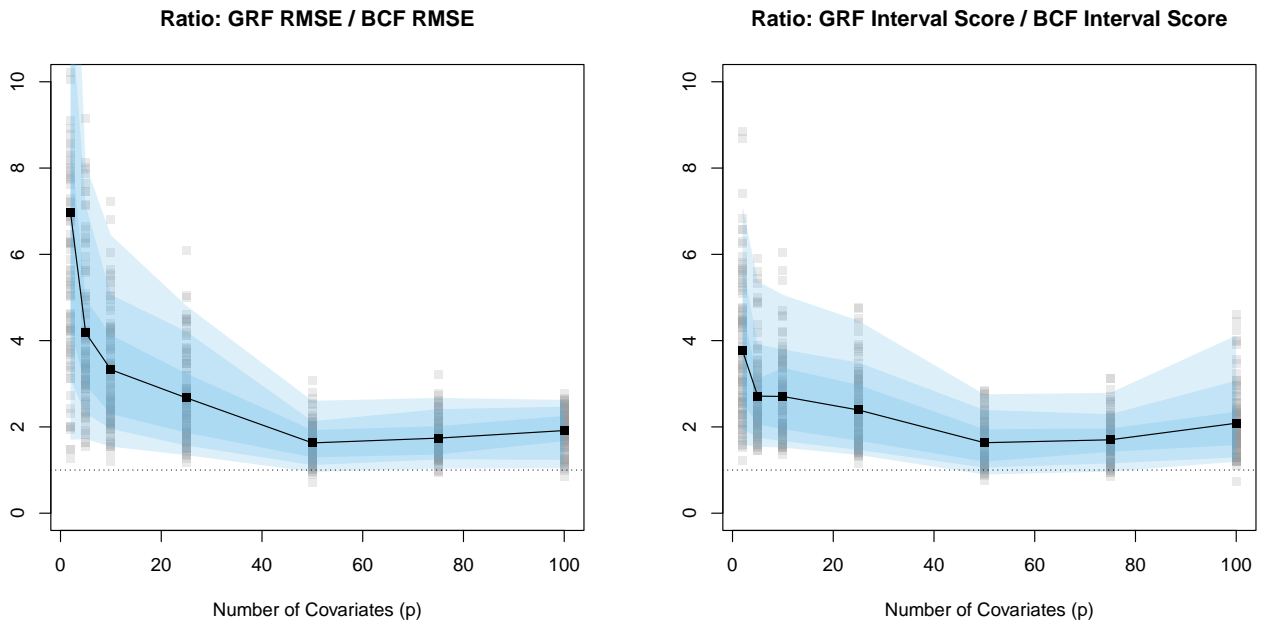


Figure 5: Comparison of BCF-LATE and GRF as the number of available covariates increases. Only two covariates are part of the simple data-generating process however, with $n = 2000$ subjects. The shaded regions correspond to the 50%, 80%, and 95% intervals across the simulations, each of which is represented with a transparent gray square. 100 simulations were performed for each distinct p , the number of covariates.

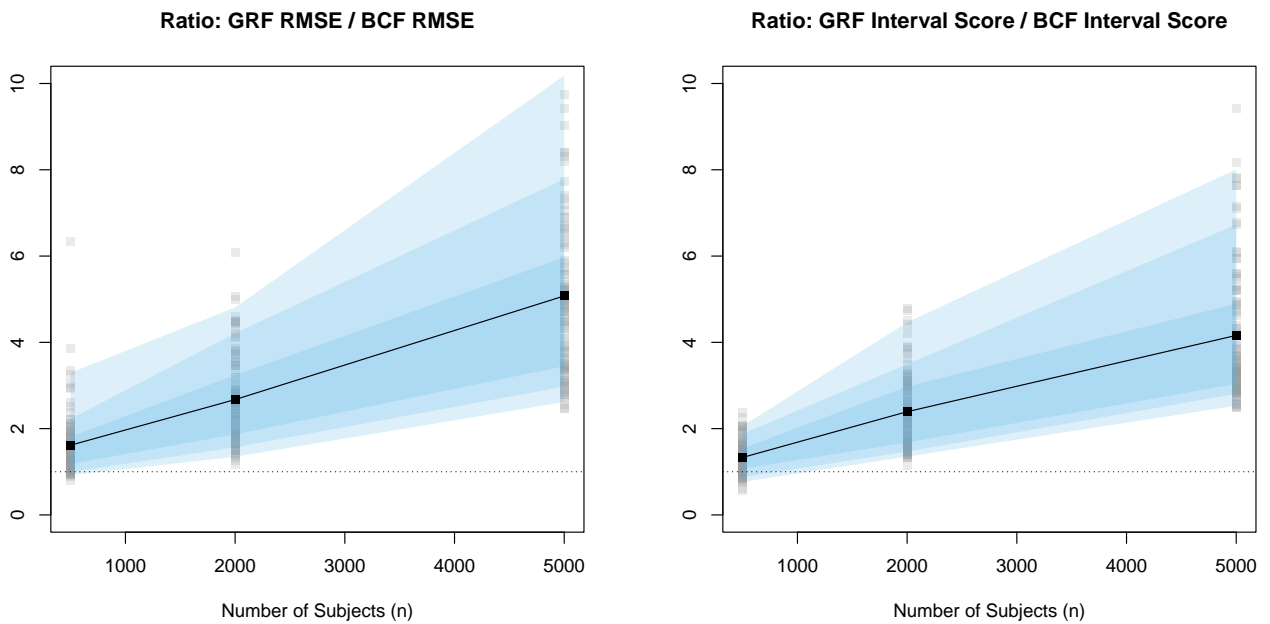


Figure 6: Comparison of BCF-LATE and GRF as the number of subjects increases. 25 covariates are provided, but only two are part of the simple data-generating process. 100 simulations were performed for each distinct n , the number of subjects.

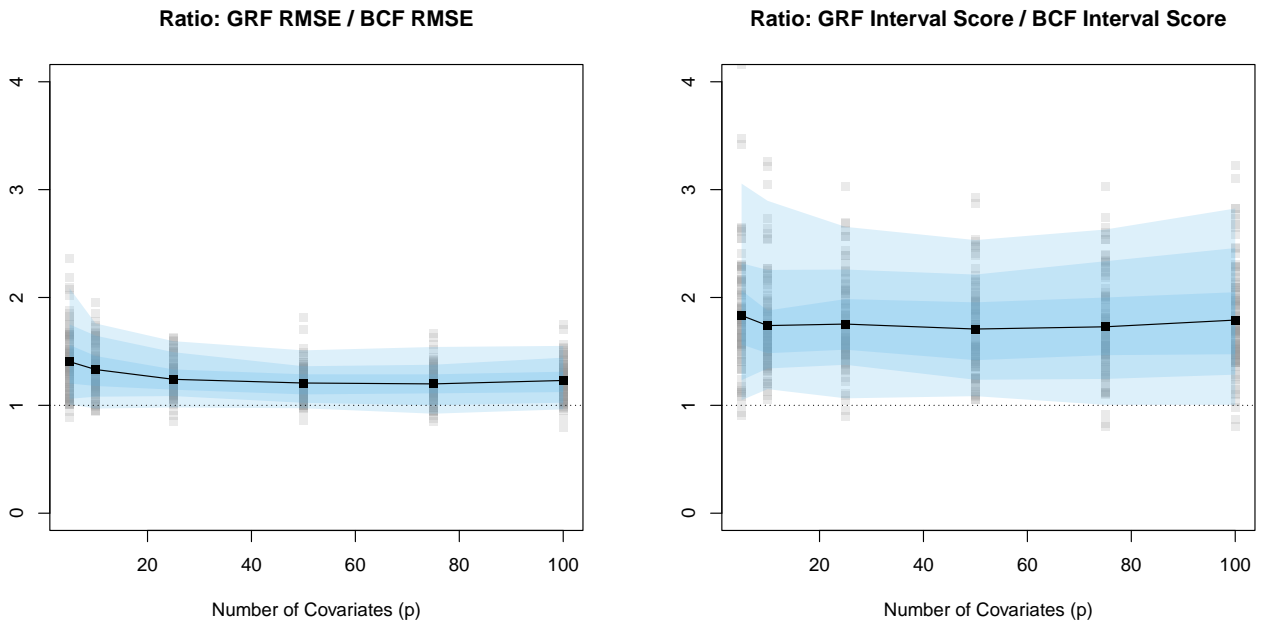


Figure 7: Comparison of BCF-LATE and GRF as the number of available covariates increases. Five covariates are part of the complicated data-generating process, with $n = 2000$ subjects. The shaded regions correspond to the 50%, 80%, and 95% intervals across the simulations, each of which is represented with a transparent gray square. 100 simulations were performed for each distinct p , the number of covariates.

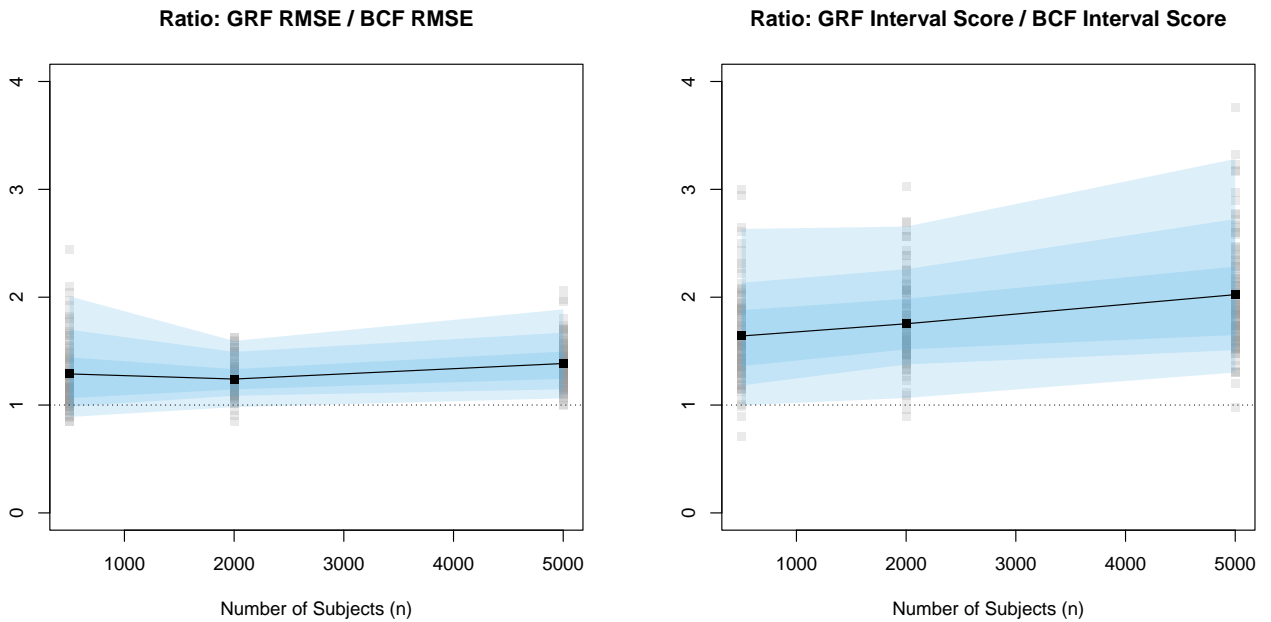


Figure 8: Comparison of BCF-LATE and GRF as the number of subjects increases. Five covariates are part of the complicated data-generating process, though 25 are provided. 100 simulations were performed for each distinct n , the number of subjects.

5 Results for Wellness Study

In this section, we apply our method to the randomized controlled trial conducted at the University of Illinois at Urbana-Champaign (Jones et al., 2019; Reif et al., 2020) called the Illinois Workplace Wellness Study. Over 12,000 employees within the university system were invited to participate, and 4,834 joined the study. At the randomization stage, 3,300 of the 4,834 were assigned to treatment and invited to participate in iThrive – the wellness program. The remaining 1,534 were not allowed to participate in iThrive and comprise the control group. Organizers offered financial awards to the treated subjects for completing the iThrive program. Hence, there are multiple sources of variation to consider. First, there is the natural variation generated from the randomization of treatment. Second, there is variation in uptake of the treatment (also known as compliance). Third, there is variation in outcomes considered. Compliance status is combination of the first two sources, and it is the second source of variation that complicates any standard differences-in-means comparison between treated and control subjects. The BCF-LATE procedure models compliance within the Bayesian causal forests framework, and we focus on a handful of binary outcomes to estimate treatment effects, uncover heterogeneity, and demonstrate the new methodology.

In the following analysis, we focus on data contained within the online surveys’ public-use data from the experiment. The data and codebooks can be found at this [link](#). Researchers conducted the survey in several annual waves. We focus on the baseline survey administered in 2016 and the first follow-up conducted in 2017. Specifically, our outcomes are survey variables measured in 2017 and displayed in Table 1. The covariates for the model are baselines values from 2016 and displayed in Table 2. All variables except for age are dichotomous, and the exact wording for a given survey question/response can be found at the [online survey study materials page](#). The age covariate is divided into three groups and described in Table 2. The final two variables considered are the treatment for subject i , A_i , and the participation of subject i in the 2016 online health risk assessment (HRA), R_i^{obs} , akin to Jones et al. (2019). This participation denotes compliance with the treatment, and of the 3,300 treated subjects, 1,848 completed the HRA. Together with the covariates and outcomes, the full quadruple of observed data is given as $(\mathbf{x}_i, A_i, R_i^{\text{obs}}, Y_i^{\text{obs}})$. Since there is missing data in the observed outcomes (and some covariates), we use the cases with complete data for each quadruple.

Table 1: Variable names and summary statistics for the **outcomes** considered. The second column is the number of non-missing observations, the third through fifth are sample statistics, and the final column is a description extracted from the survey data codebook. All outcomes have missing observations since the sample sizes are less than the entire experimental group of 4,834. The mean statistics represent the average number of “1’s” across available observations since all outcomes are binary variables.

Outcomes	N	Mean	Min	Max	Description
chronic_0717	3565	0.73	0	1	Has at least 1 chronic condition (2017)
badhealth_0717	3567	0.32	0	1	High blood pressure, cholesterol, or glucose (2017)
mgmtsafety_0717	3566	0.79	0	1	Management places very high or some priority on health/safety (2017)

We now demonstrate the BCF-LATE methodology on this data. For each outcome, we run the sampler with 5,000 burn-in and 10,000 MCMC posterior draws. The estimated LATE(x) for each outcome is the posterior mean of these draws, computed over each subject in our sample. These subject-specific LATEs are also called conditional LATEs or CLATEs. With the CLATE estimates in hand, we display two figures for each outcome in Figures 9, 11, and 13. The left-hand panel of each figure is the CLATE distribution of subjects in the sample, and the right panel is a summary tree of the distribution’s modes in terms of the original covariates. We obtain this summary using a shallow regression tree model, following the advice in Hahn et al. (2020). We fit a Classification and Regression Tree (CART) where the outcome is the subject-specific posterior mean CLATE, and the predictors are the original covariates. This summarization step produces a parsimonious description of CLATEs by splitting on covariates describing subgroups with the most meaningful heterogeneity. The process of summarizing a complex posterior enjoys a robust and growing

literature base, including [Hahn and Carvalho \(2015\)](#), [Puelz et al. \(2017\)](#), [Fisher et al. \(2020\)](#), and [Bolfarine et al. \(2024\)](#). Often called “fitting the fit” since its input is a model fit and output is the fit’s summarization, there is not one unique way to undertake the posterior summary step. Thus, we rely on existing work on heterogeneous treatment effect summarization for this analysis. The right panels of Figures 9, 11, and 13 show the average subgroup CLATE in the node, and the percentage of the sample beneath the node. A left split on each decision rule affirms the rule, while a right split negates the rule. As a final note before diving into each individual outcome, we show the posterior credible intervals for each discovered subgroup’s LATE in Figures 10, 12, and 14. These intervals provide information on whether treatment effects contain significant posterior mass away from zero.

Table 2: Variable names and summary statistics for the **covariates** considered. These are the baseline survey values obtained in 2016. The second column is the number of non-missing observations, the third through fifth are sample statistics, and the final column is a description extracted from the survey data codebook. The mean statistics represent the average number of “1’s” across available observations since all outcomes are binary variables except for the “age” covariate.

Covariates	N	Mean	Min	Max	Description
male	4834	0.43	0	1	Male indicator
age	4834	0.99	0	2	0 = less than 37, 1 = 37-49, 2 = greater than 49
white	4834	0.84	0	1	White race indicator
everscreen_0716	4834	0.89	0	1	Had at least 1 previous health screening (2016)
active_0716	4834	0.37	0	1	Physically active (2016)
active_try_0716	4834	0.81	0	1	Trying to be more active (2016)
curismk_0716	4833	0.07	0	1	Current smoker (2016)
othersmk_0716	4833	0.09	0	1	Other (non-cigarette) tobacco use (2016)
formsmk_0716	4833	0.20	0	1	Former smoker (2016)
drink_0716	4830	0.65	0	1	Drinker (2016)
drinkhvy_0716	4829	0.05	0	1	Heavy drinker (2016)
chronic_0716	4834	0.73	0	1	Has at least 1 chronic condition (2016)
health1_0716	4834	0.60	0	1	Health is excellent or very good (2016)
health2_0716	4834	0.99	0	1	Health is not poor (2016)
problems_0716	4834	0.39	0	1	Problems with physical activities or pain (2016)
energy_0716	4834	0.32	0	1	Lots of energy (2016)
ehealth_0716	4834	0.29	0	1	Emotional health (2016)
overweight_0716	4834	0.54	0	1	Overweight status (2016)
badhealth_0716	4834	0.30	0	1	High blood pressure, cholesterol, or glucose (2016)
sedentary_0716	4833	0.54	0	1	Sedentary job (2016)
druguse_0716	4830	0.71	0	1	Taking 1+ prescription/OTC drugs (2016)
physician_0716	4833	0.76	0	1	Physician or ER utilization (2016)
hospital_0716	4833	0.03	0	1	Hospital utilization (2016)
sickdays_0716	4828	0.61	0	1	Sick days in past 12 months (baseline survey) (2016)
hrsworked50_0716	4831	0.18	0	1	Worked 50 or more hours per week (2016)
jobsatisf1_0716	4832	0.40	0	1	Very satisfied with job (2016)
jobsatisf2_0716	4832	0.84	0	1	Very or somewhat satisfied with job (2016)
mgmtsafety_0716	4831	0.78	0	1	Management places very high or some priority on health/safety (2016)

Figure 9 displays the results for the outcome of whether or not the subject has at least one chronic health condition in 2017. This CLATE distribution contains one prominent mode centered around a negative but negligible treatment effect (-0.0017). However, the summary tree splits on covariates in symmetric positive and negative directions. It first splits on whether baseline health is excellent or very good. Specifically, the left split leads to a negative treatment effect (-0.011), meaning that subjects with baseline health not excellent or very good saw the treatment effect of the wellness program decrease the probability of a chronic condition in 2017 by 1.1 percentage points. The most granular subgroups are at the bottom nodes, and we can interpret the far-left subgroup as follows. Study subjects who:

- rate their baseline health as not excellent or very good,
- are white,
- did not have a chronic health condition at baseline,

see an estimated 2.8 percentage point *decrease* in the chance of at least one chronic health condition in 2017 due to the wellness program. On the other hand, study subjects who:

- rate their baseline health as excellent or very good,
- are not white,
- did not have high blood pressure, cholesterol, or glucose at baseline,

see an estimated 2.4 percentage point *increase* in the chance of at least one chronic health condition in 2017 due to the wellness program. This subgroup estimate is given in the far-right node in Figure 9. The posterior uncertainty about the far-left and right subgroups is large, i.e., there is mass above and below zero (see the bottom and top intervals of Figure 10, respectively) which indicates there is not much heterogeneity or significant impact of the intervention on this particular survey outcome. This result matches the null result on the chronic condition outcome in Jones et al. (2019).

The second outcome considered is whether or not the subject has elevated blood pressure, cholesterol, or glucose in 2017. The results are displayed in Figure 11. The distribution of CLATEs in this case is interesting for two reasons. First, there is clear heterogeneity in the treatment effect of the wellness program since there are two distinct modes around small negative and moderately positive values (left panel in Figure 11). Second, most subgroup effects are positive, suggesting that the wellness program increases the chance of elevated blood pressure, cholesterol, or glucose in the following year. At first glance, this is counterintuitive at best and dismaying at worst. However, the subgroups defined in the summary tree (Figure 11) hint at what could be driving this result. The first split in the summary tree demarcating the two modes happens on the baseline elevated blood pressure / cholesterol / glucose covariate, “badhealth_0716.”

The survey question defining this covariate is related to health perception: *How would you describe your blood pressure / cholesterol / glucose level? That is, if we measured it right now, do you think your blood pressure level would be: ...* (see survey questions [here](#)). The positive treatment effect subgroup are those subjects who say their levels for these metrics are “low” or “normal” (Jones et al., 2019). In other words, they are optimistic about their health status. Interpreting the far-right node in the summary tree, the group with the highest chance of elevated “bad health metrics” in 2017 are those who were previously optimistic at baseline (first split), male (second split), and overweight at baseline (third split). The wellness program increases this subgroup’s chance of elevated “bad health metrics” by 7.4 percentage points. In summary, this baseline optimism appears to drive the positive treatment effect. There is research supporting this divergence of health perception versus reality in psychological theory (Rosenstock et al., 1988) and empirical psychology (Dalbo et al., 2017). The BCF-LATE methodology reveals this interesting phenomenon in the survey data by clearly describing heterogeneity in the wellness program’s treatment effects. Figure 12 demonstrates significance of these subgroup effects. Most of the posterior mass for the fifth through eighth subgroups (right four subgroups in Figure 11) is above zero, providing evidence the intervention increases the chance of a bad health outcome after one year for those without preexisting “bad health.” The combined 90% credible

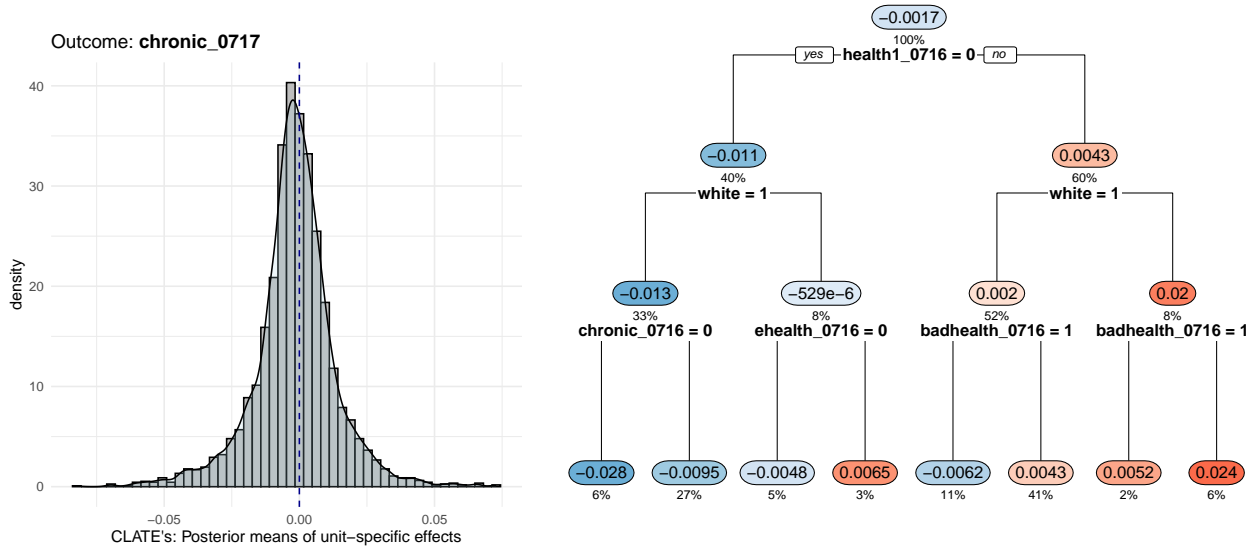


Figure 9: Posterior means of CLATEs (left) and summary tree of CLATE distribution (right). The outcome modeled is chronic.0717, which is equal to one if the subject has at least one chronic medical condition in 2017. The summary tree on the right splits on baseline covariates from 2016. The numbers within the nodes are the subgroup average CLATEs (in units of percentage), and the numbers below the nodes are the subgroups' percentage of the sample. The node colors are red for positive, blue for negative, and shades of white for close to zero in absolute value.

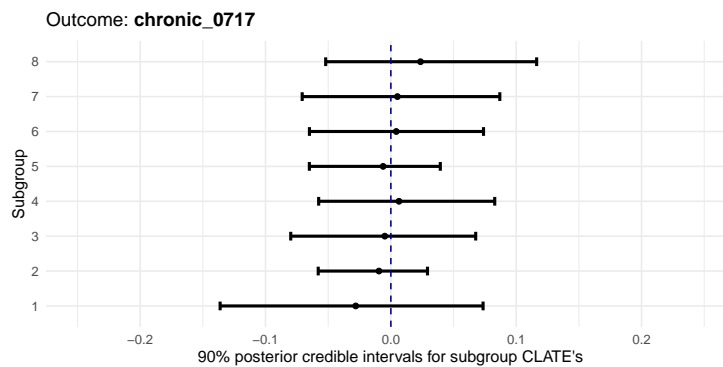


Figure 10: Posterior credible intervals of the subgroup CLATEs for the 8 subgroups represented in the summary tree leaves in Figure 9 (right). The bars are the 90% intervals, and the dots are the posterior means. The bottom interval (subgroup 1) corresponds to the far-left leaf and the top interval (subgroup 8) corresponds to the far-right leaf in Figure 9 (right). The interior intervals for subgroups 2 through 7 match the interior leaves, respectively.

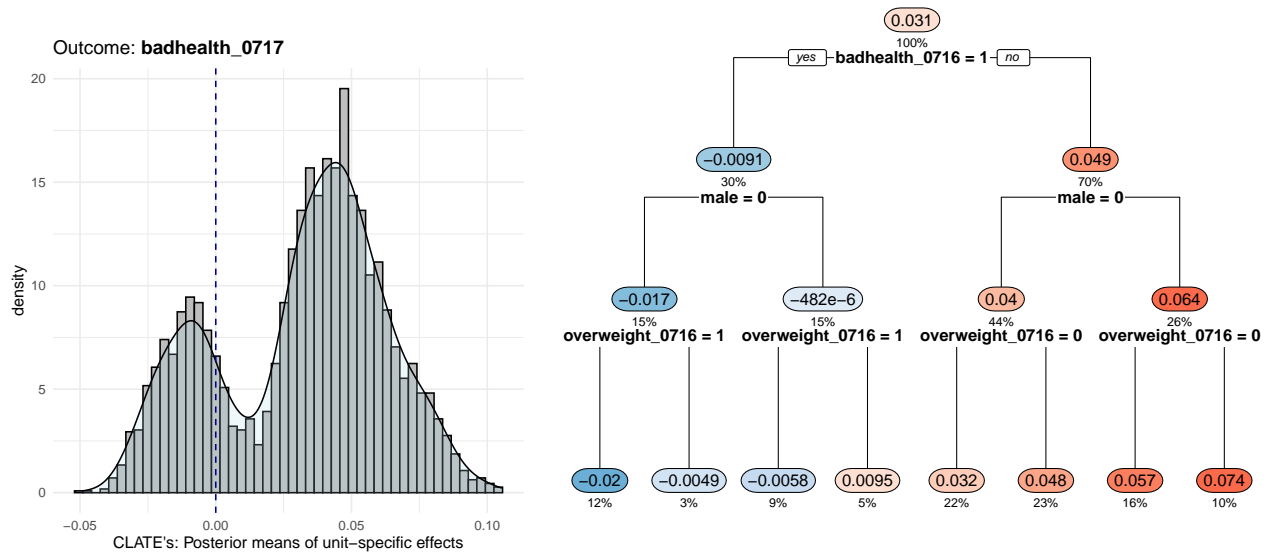


Figure 11: Posterior means of CLATEs (left) and summary tree of CLATE distribution (right). The outcome modeled is badhealth_0717, which is equal to one if the subject perceives their blood pressure, cholesterol, or glucose levels to be elevated, i.e., a negative health outcome. The summary tree on the right splits on baseline covariates from 2016. The numbers within the nodes are the subgroup average CLATEs (in units of percentage), and the numbers below the nodes are the subgroups' percentage of the sample. The node colors are red for positive, blue for negative, and shades of white for close to zero in absolute value.

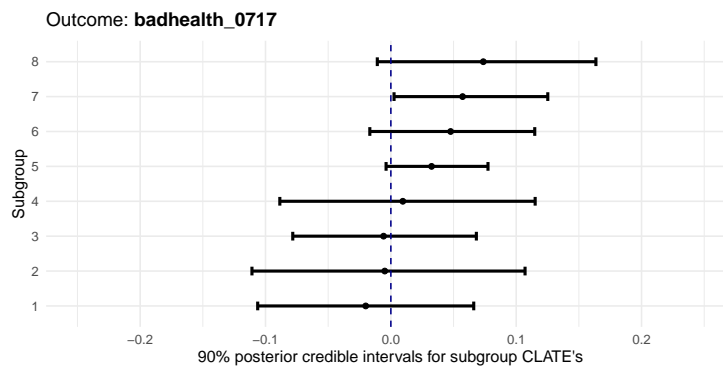


Figure 12: Posterior credible intervals of the subgroup CLATEs for the 8 subgroups represented in the summary tree leaves in Figure 11 (right). The bars are the 90% intervals, and the dots are the posterior means. The bottom interval (subgroup 1) corresponds to the far-left leaf and the top interval (subgroup 8) corresponds to the far-right leaf in Figure 11 (right). The interior intervals for subgroups 2 through 7 match the interior leaves, respectively.

interval for subgroups five through eight is $(-0.007, 0.122)$. Two questions of significance should arise: 1) are the subgroups' effects actually different and 2) are the effects nonzero. The sample LATE for individuals who did not report these health problems in the Summer of 2016 has a 0.9239 posterior probability of being positive (the right mode in Figure 11), while those who did report health issues (the left mode) have a 0.4201 posterior probability of a positive LATE. Furthermore, there is a 0.9276 posterior probability that these two LATEs are different. Therefore, we can say that there is evidence that these two subgroups' LATEs are heterogeneous, and that there is evidence that one of the subgroups' LATE is larger than zero. This heterogeneity adds depth to the first-year treatment effects presented in Jones et al. (2019), which, like the first outcome, do not find a significant treatment effect for the bad health outcome.

The final outcome surveys whether “management places very high or some priority on health/safety.” The treatment effects and discovered subgroups are displayed in the left and right of Figure 13, respectively. The CLATE distribution displays a remarkable amount of heterogeneity with at least four well-defined modes, underscoring the advantage of using the BCF-LATE modeling approach. All subgroup effects are positive, indicating that the intervention increases the probability an individual will answer management prioritizes their health/safety one year after program participation. The summary tree splits on baseline sick days taken, overweight status, job satisfaction, and management health/safety prioritization. Notably, the largest positive subgroup effects are significant with the majority of the posterior mass above zero. Indeed, three out of the four subgroups on the right of the summary tree have 90% posterior credible interval that do not cover zero, as seen on Figure 14. The four different modes seen in the left pane of Figure 13 line up fairly well with the four subgroups found in the third level of the tree in the right pane. We find that the subgroups with the larger LATE estimates (the right side of the tree, comprised of individuals who did not feel as though they had tons of energy in 2016) have more than 0.96 posterior probability of having positive LATEs. Furthermore, the far-right subgroup of the four (do not self-report lots of energy and do not have high opinions of management's priority on health and safety) has more than 0.99 posterior probability of having a larger LATE than the other subgroups. This result is in line with the analysis in Jones et al. (2019), where they find a significant first-year treatment effect on the management prioritization outcome. The BCF-LATE bolsters this finding by uncovering heterogeneity among the subjects' effect sizes and shows which individuals within the sample drive this positive effect.

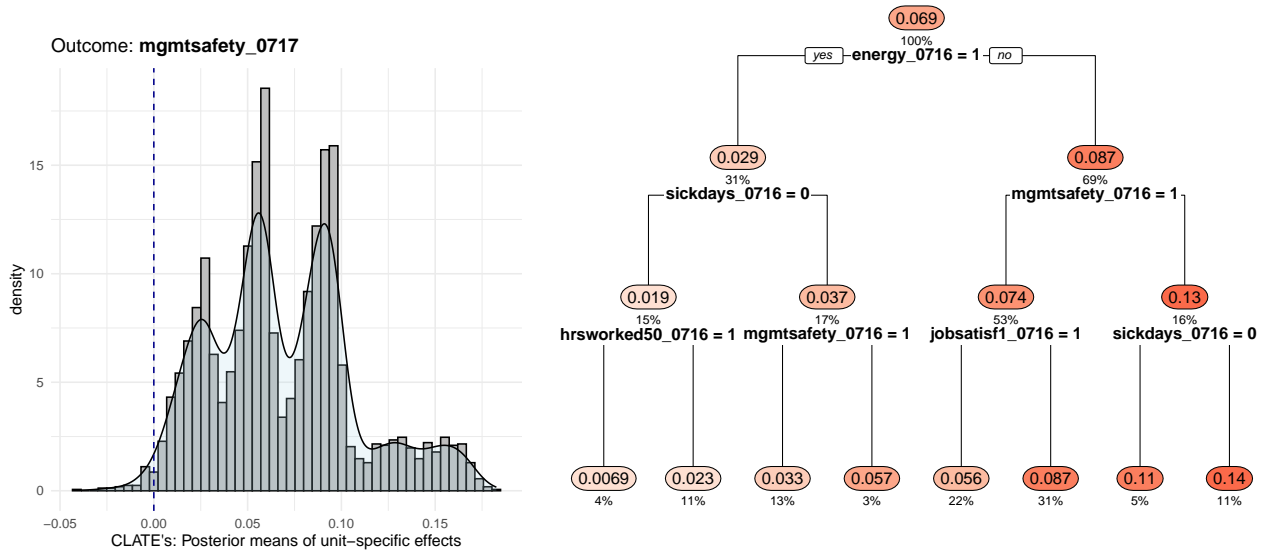


Figure 13: Posterior means of CLATEs (left) and summary tree of CLATE distribution (right). The outcome modeled is mgmtsafety_0717, which is equal to one if the subject believes management prioritizes health and safety. The summary tree on the right splits on baseline covariates from 2016. The numbers within the nodes are the subgroup average CLATEs (in units of percentage), and the numbers below the nodes are the subgroups' percentage of the sample. The node colors are red for positive, blue for negative, and shades of white for close to zero in absolute value.

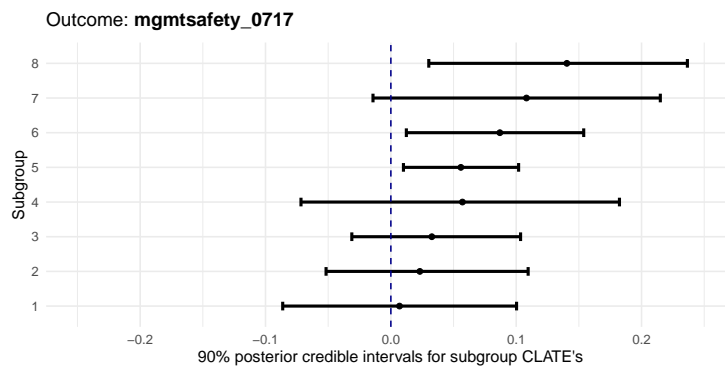


Figure 14: Posterior credible intervals of the subgroup CLATEs for the 8 subgroups represented in the summary tree leaves in Figure 13 (right). The bars are the 90% intervals, and the dots are the posterior means. The bottom interval (subgroup 1) corresponds to the far-left leaf and the top interval (subgroup 8) corresponds to the far-right leaf in Figure 13 (right). The interior intervals for subgroups 2 through 7 match the interior leaves, respectively.

6 Discussion

In this paper we have proposed an extension of the Bayesian Causal Forest model (BCF) to account for one-sided noncompliance when outcomes of interest are binary. Our approach includes modeling compliance jointly with the outcome using nonlinear functions from Bayesian additive regression trees (BART [Chipman et al., 2010](#)). We have shown that by modeling compliance, our method performs better than traditional methods when compliance rates are low/the instrument is weak.

Using our method to analyze the Illinois Workplace Wellness Study ([Jones et al., 2019](#); [Reif et al., 2020](#)), we find that the conditional local average treatment effects vary for certain binary outcomes. Specifically, we find heterogeneity in the impact of the workplace wellness intervention on compliers’ rates of certain self-reported health issues. Compliers who did not report high blood pressure, cholesterol, or glucose were more likely to report it the following year if they were randomized to the wellness plan. This may be counter-intuitive that the rate went up due to healthy behaviors, but given that the change happened within 12 months, it seems most likely this can be attributed to pre-existing issues that were discovered because healthy behaviors were taken up. Similarly, we find that while employees’ views about management’s priority on health and safety have a significant local average treatment effect like in [Jones et al. \(2019\)](#), we also see that there are subgroups of interest with varying magnitudes of effects.

Two future extensions are evident. First, our work here has been for one-sided noncompliance when the outcome is binary. Two-sided noncompliance usually has three latent strata (four if the monotonicity assumption does not hold), and this would require the compliance model to be multinomial. [Chen et al. \(2024\)](#) approached this with two nested probit models, though they were looking at survival analysis instead of treatment compliance. This could also be done with the loglinear multinomial BART model of [Murray \(2021\)](#) or with the general BART methods of [Linero \(2024\)](#).

Second, Assumption [A1](#), “SUTVA”, implies that there is no interference across units, but because all employees were invited, there likely are peer effects. The original authors of [Jones et al. \(2019\)](#) are working on this currently, though another future direction can explore treatment effect heterogeneity while also accounting for the interference over the network of people. Furthermore, the dollar amounts offered as the incentive to participate in the program were also randomized, though we proceed as the original paper [Jones et al. \(2019\)](#) did and consider this a single treatment.

Acknowledgements

We would like to thank Julian Reif, David Molitor, and Damon Jones for their advice with the data from their works ([Jones et al., 2019](#); [Reif et al., 2020](#)). We would also like to thank Jared Murray and Avi Feller for their ideas and support on the early variants of this project and Hyunseung Kang for several helpful discussions.

References

- Albert, J. H. and Chib, S. (1993). Bayesian analysis of binary and polychotomous response data. *Journal of the American Statistical Association*, 88(422):669–679.
- Andrews, I., Stock, J. H., and Sun, L. (2019). Weak instruments in instrumental variables regression: Theory and practice. *Annual Review of Economics*, 11(1):727–753.
- Angrist, J. D., Imbens, G. W., and Rubin, D. B. (1996). Identification of causal effects using instrumental variables. *Journal of the American Statistical Association*, 91(434):444–455.
- Angrist, J. D. and Pischke, J.-S. (2009). *Mostly harmless econometrics: An empiricist’s companion*. Princeton University Press.
- Athey, S., Tibshirani, J., and Wager, S. (2019). Generalized random forests. *Annals of Statistics*, 47(42):1148–1178.

- Athey, S. and Wager, S. (2019). Estimating treatment effects with causal forests: An application. *Observational Studies*, 5(2):37–51.
- Bargagli-Stoffi, F. J., De Witte, K., and Gnecco, G. (2022). Heterogeneous causal effects with imperfect compliance: A Bayesian machine learning approach. *The Annals of Applied Statistics*, 16(3):1986–2009.
- Bolfarine, H., Carvalho, C. M., Lopes, H. F., and Murray, J. S. (2024). Decoupling shrinkage and selection in gaussian linear factor analysis. *Bayesian Analysis*, 19(1):181–203.
- Chen, X., Harhay, M. O., Tong, G., and Li, F. (2024). A Bayesian machine learning approach for estimating heterogeneous survivor causal effects: Applications to a critical care trial. *The Annals of Applied Statistics*, 18(1):350–374.
- Chipman, H. A., George, E. I., and McCulloch, R. E. (1998). Bayesian CART model search. *Journal of the American Statistical Association*, 93(443):935–948.
- Chipman, H. A., George, E. I., and McCulloch, R. E. (2010). BART: Bayesian additive regression trees. *The Annals of Applied Statistics*, 4(1):266 – 298.
- Dalbo, V. J., Teramoto, M., Roberts, M. D., and Scanlan, A. T. (2017). Lack of reality: Positive self-perceptions of health in the presence of disease. *Sports*, 5(2):23.
- Deshpande, S. K., Bai, R., Balocchi, C., Starling, J. E., and Weiss, J. (2024). VCBART: Bayesian trees for varying coefficients. *arXiv preprint arXiv:2003.06416*.
- Fisher, J. D., Puelz, D. W., and Carvalho, C. M. (2020). Monotonic effects of characteristics on returns. *The Annals of Applied Statistics*, 14(4):1622 – 1650.
- Frangakis, C. E. and Rubin, D. B. (2002). Principal stratification in causal inference. *Biometrics*, 58(1):21–29.
- Gneiting, T. and Raftery, A. E. (2007). Strictly proper scoring rules, prediction, and estimation. *Journal of the American Statistical Association*, 102(477):359–378.
- Hahn, P. R. and Carvalho, C. M. (2015). Decoupling shrinkage and selection in Bayesian linear models: a posterior summary perspective. *Journal of the American Statistical Association*, 110(509):435–448.
- Hahn, P. R., Murray, J. S., and Carvalho, C. M. (2020). Bayesian regression tree models for causal inference: Regularization, confounding, and heterogeneous effects (with discussion). *Bayesian Analysis*, 15(3):965–1056.
- Hill, J. L. (2011). Bayesian nonparametric modeling for causal inference. *Journal of Computational and Graphical Statistics*, 20(1):217–240.
- Imbens, G. W. and Rubin, D. B. (2015). *Causal inference in statistics, social, and biomedical sciences*. Cambridge University Press.
- Johnson, M., Cao, J., and Kang, H. (2022). Detecting heterogeneous treatment effects with instrumental variables and application to the Oregon health insurance experiment. *The Annals of Applied Statistics*, 16(2):1111–1129.
- Jones, D., Molitor, D., and Reif, J. (2019). What do Workplace Wellness Programs do? Evidence from the Illinois Workplace Wellness Study*. *The Quarterly Journal of Economics*, 134(4):1747–1791.
- Kim, C. and Zigler, C. (2024). Bayesian nonparametric trees for principal causal effects. *arXiv preprint arXiv:2403.13256*.
- Künzel, S. R., Sekhon, J. S., Bickel, P. J., and Yu, B. (2019). Metalearners for estimating heterogeneous treatment effects using machine learning. *Proceedings of the National Academy of Sciences*, 116(10):4156–4165.
- Levy, D. E. and Thorndike, A. N. (2019). Workplace wellness program and short-term changes in health care expenditures. *Preventive Medicine Reports*, 13:175–178.
- Linero, A. R. (2018). Bayesian regression trees for high-dimensional prediction and variable selection. *Journal of the American Statistical Association*, 113(522):626–636.

- Linero, A. R. (2024). Generalized Bayesian additive regression trees models: Beyond conditional conjugacy. *Journal of the American Statistical Association*, pages 1–14.
- McCulloch, R. E., Sparapani, R. A., Logan, B. R., and Laud, P. W. (2021). Causal inference with the instrumental variable approach and bayesian nonparametric machine learning. *arXiv preprint arXiv:2102.01199*.
- Mulaney, B., Bromley-Dulfano, R., Stepanek, E. K. M. M., and Singer, S. J. (2021). Descriptive study of employee engagement with workplace wellness interventions in the UK. *Journal of Occupational and Environmental Medicine*, 63(9):719–730.
- Murray, J. S. (2021). Log-linear Bayesian additive regression trees for multinomial logistic and count regression models. *Journal of the American Statistical Association*, 116(534):756–769.
- Page, L. C., Feller, A., Grindal, T., Miratrix, L., and Somers, M.-A. (2015). Principal stratification: A tool for understanding variation in program effects across endogenous subgroups. *American Journal of Evaluation*, 36(4):514–531.
- Puelz, D., Hahn, P. R., and Carvalho, C. M. (2017). Variable Selection in Seemingly Unrelated Regressions with Random Predictors. *Bayesian Analysis*, 12(4):969 – 989.
- Ratkovic, M. and Shiraito, Y. (2014). Strengthening weak instruments by modeling compliance. In *Annual Meeting of the Midwest Political Science Association*.
- Reif, J., Chan, D., Jones, D., Payne, L., and Molitor, D. (2020). Effects of a workplace wellness program on employee health, health beliefs, and medical use: A randomized clinical trial. *JAMA Internal Medicine*, 180(7):952–960.
- Rosenstock, I. M., Strecher, V. J., and Becker, M. H. (1988). Social learning theory and the health belief model. *Health Education Quarterly*, 15(2):175–183.
- Song, Z. and Baicker, K. (2021). Health and economic outcomes up to three years after a workplace wellness program: A randomized controlled trial: Study examines the health and economic outcomes of a workplace wellness program. *Health Affairs*, 40(6):951–960.
- Wager, S. and Athey, S. (2018). Estimation and inference of heterogeneous treatment effects using random forests. *Journal of the American Statistical Association*, 113(523):1228–1242.
- Wald, A. (1940). The fitting of straight lines if both variables are subject to error. *The Annals of Mathematical Statistics*, 11(3):284–300.
- Wright, P. G. (1928). *The tariff on animal and vegetable oils*. Number 26. Macmillan.

A Gibbs Sampler Derivation

To derive our Gibbs sampler, we introduce some additional notation. Given a regression tree (T, \mathcal{B}) and a point \mathbf{x} , let $\ell(\mathbf{x}; T)$ be the leaf of T associated with \mathbf{x} . Further, let $g(\mathbf{x}; T, \mathcal{B})$ be the evaluation function that returns the jump associated with $\ell(\mathbf{x}; T)$; that is

$$g(\mathbf{x}; T, \mathcal{B}) = \beta_{\ell(\mathbf{x}; T)}.$$

With this notation, we can write

$$\mu(\mathbf{x}) = \sum_{m=1}^{M_\mu} g(\mathbf{x}; T_m^{(\mu)}, \mathcal{B}_m^{(\mu)}).$$

We can analogously express each of $\mu_c(\mathbf{x})$, $\tau(\mathbf{x})$, and $\eta(\mathbf{x})$ as sums of tree evaluations. Finally, let $\Theta = \{\theta^{(\mu)}, \theta^{\mu_c}, \theta^{(\tau)}, \theta^{(\eta)}\}$ denote the collection of prior variable splitting probabilities.

A.1 Sampling latent utilities and missing compliance statuses

Each iteration of our Gibbs sampler begins by first sampling the missing compliance statuses $\mathbf{C}^{(0)}$ and then drawing latent utilities \tilde{Y}_i and \tilde{C}_i for each subject.

The joint conditional density of unobserved compliance statuses for control subjects is given by

$$\begin{aligned} p(\mathbf{C}^{(0)} | \mathbf{Y}, \mathcal{E}) \propto & \prod_{i: a_i=0} \left\{ [\Phi(\mu(\mathbf{x}_i) + \mu_c(\mathbf{x}_i) \times c_i)]^{y_i} \times [1 - \Phi(\mu(\mathbf{x}) + c_i \times \mu_c(\mathbf{x}))]^{1-y_i} \right\} \\ & \times \prod_{i: a_i=0} \left\{ \Phi(\eta(\mathbf{x}))^{c_i} \times [1 - \Phi(\eta(\mathbf{x}_i))]^{1-c_i} \right\}. \end{aligned} \quad (\text{A13})$$

From (A13) we can conclude that the latent compliance statuses are conditionally independent given \mathcal{E} (which determines the functions μ , μ_c , τ , and η) and the observed outcomes \mathbf{Y} . We further compute

$$\mathbb{P}(C_i = 1 | Y_i = 1, \mathcal{E}) = \frac{\Phi(\eta(\mathbf{x})) \times \Phi(\mu(\mathbf{x}_i) + \mu_c(\mathbf{x}_i))}{\Phi(\eta(\mathbf{x})) \times \Phi(\mu(\mathbf{x}_i) + \mu_c(\mathbf{x}_i)) + (1 - \Phi(\eta(\mathbf{x}))) \times \Phi(\mu(\mathbf{x}_i))}. \quad (\text{A14})$$

$$\mathbb{P}(C_i = 1 | Y_i = 0, \mathcal{E}) = \frac{\Phi(\eta(\mathbf{x})) \times (1 - \Phi(\mu(\mathbf{x}_i) + \mu_c(\mathbf{x}_i)))}{\Phi(\eta(\mathbf{x})) \times (1 - \Phi(\mu(\mathbf{x}_i) + \mu_c(\mathbf{x}_i))) + (1 - \Phi(\eta(\mathbf{x}))) \times (1 - \Phi(\mu(\mathbf{x}_i)))}$$

So, in the first step of each Gibbs sampling iteration, we sample a new value of $\mathbf{C}^{(0)}$ by independently drawing C_i 's according to Equation (A14).

Having drawn the missing compliance statuses, our data likelihood is now

$$p(\mathbf{Y}, \mathbf{C} | \mathcal{E}) \propto \prod_{i=1}^n \left[\Phi(f(\mathbf{x}_i, c_i, a_i))^{y_i} \times (1 - \Phi(f(\mathbf{x}_i, c_i, a_i)))^{1-y_i} \times \Phi(\eta(\mathbf{x}_i))^{c_i} \times (1 - \Phi(\eta(\mathbf{x}_i)))^{1-c_i} \right].$$

Following [Albert and Chib \(1993\)](#), we introduce latent utilities \tilde{Y}_i and \tilde{C}_i such that $Y_i = \mathbb{1}(\tilde{Y}_i \geq 0)$ and $C_i = \mathbb{1}(\tilde{C}_i \geq 0)$, yielding the augmented likelihood

$$\begin{aligned} p(\mathbf{Y}, \mathbf{C}, \tilde{\mathbf{Y}}, \tilde{\mathbf{C}} | \mathcal{E}) \propto & \exp \left\{ -\frac{1}{2} \sum_{i=1}^n (\tilde{y}_i - f(\mathbf{x}_i, c_i, a_i))^2 \right\} \times \prod_{i=1}^n \mathbb{1}(Y_i = \mathbb{1}(\tilde{Y}_i \geq 0)) \\ & \times \exp \left\{ -\frac{1}{2} \sum_{i=1}^n (\tilde{c}_i - \eta(\mathbf{x}_i))^2 \right\} \times \prod_{i=1}^n \mathbb{1}(C_i = \mathbb{1}(\tilde{C}_i \geq 0)). \end{aligned} \quad (\text{A15})$$

From Equation (A15), we conclude that

$$\tilde{Y}_i \sim \mathbb{1}(Y_i = 1) \times \mathcal{N}_+(f(\mathbf{x}_i, c_i, a_i), 1) + \mathbb{1}(Y_i = 0) \times \mathcal{N}_-(f(\mathbf{x}_i, c_i, a_i), 1) \quad (\text{A16})$$

$$\tilde{C}_i \sim \mathbb{1}(S_i = 1) \times \mathcal{N}_+(\eta(\mathbf{x}_i), 1) + \mathbb{1}(C_i = 0) \times \mathcal{N}_-(\eta(\mathbf{x}_i), 1), \quad (\text{A17})$$

where \mathcal{N}_+ and \mathcal{N}_- respectively denote truncations of a normal distribution to the positive and negative axes. The second step of each Gibbs sampling iteration begins by drawing latent utilities \tilde{Y}_i and \tilde{C}_i for each $i = 1, \dots, n$ according to Equations (A16) and (A17).

A.2 Updating regression trees

Once we draw the latent utilities $\tilde{\mathbf{Y}}$ and $\tilde{\mathbf{C}}$, we sweep over the trees in \mathcal{E} , updating them one at a time conditionally on the fits of all other trees and the latent variables. Each update involves sampling a regression tree (T, \mathcal{B}) from a particular conditional distribution whose density is of the form

$$p(T, \mathcal{B} | \tilde{\mathbf{Y}}, \tilde{\mathbf{C}}, \mathcal{E}^-) \propto p(T)p(\mathcal{B} | T)p(\tilde{\mathbf{Y}}, \tilde{\mathbf{C}} | T, \mathcal{B}, \mathcal{E}^-), \quad (\text{A18})$$

where \mathcal{E}^- denotes the collection of all other regression trees. We draw trees from such distributions in two steps. First, we sample the decision tree T from the corresponding marginal distribution. This is done using a variant of the Metropolis-Hastings approach introduced by Chipman et al. (1998) that only implements grow and prune moves. Then we sample $\mathcal{B} | T$ from its corresponding conditional.

From Equation (A15), that the ‘‘likelihood’’ term $p(\tilde{\mathbf{Y}}, \tilde{\mathbf{C}} | T, \mathcal{B}, \mathcal{E}^-)$ depends on $\tilde{\mathbf{Y}}$ and $\tilde{\mathbf{C}}$ through the *full residuals*

$$\begin{aligned} R_i^{(y)} &= \tilde{y}_i - f(\mathbf{x}_i, c_i, a_i) \\ R_i^{(c)} &= \tilde{c}_i - \eta(\mathbf{x}_i). \end{aligned}$$

Updating $\mathcal{E}^{(\mu)}$. To update the m -th tree $(T_m^{(\mu)}, \mathcal{B}_m^{(\mu)})$ in $\mathcal{E}^{(\mu)}$, we set

$$p(\tilde{\mathbf{Y}}, \tilde{\mathbf{C}} | T, \mathcal{B}, \mathcal{E}^-) = \exp \left\{ -\frac{1}{2} \left[\sum_{i=1}^n (r_i^{(\mu)} - g(\mathbf{x}_i; T, \mathcal{B}))^2 \right] \right\}, \quad (\text{A19})$$

where $r_i^{(\mu)}$ is the partial residual

$$r_i^{(\mu)} = R_i^{(y)} + g(\mathbf{x}_i; T_m^{(\mu)}, \mathcal{B}_m^{(\mu)}). \quad (\text{A20})$$

Updating $\mathcal{E}^{(\mu_c)}$. To update the m -th tree $(T_m^{(\mu_c)}, \mathcal{B}_m^{(\mu_c)})$ in $\mathcal{E}^{(\mu_c)}$, we set

$$p(\tilde{\mathbf{Y}}, \tilde{\mathbf{C}} | T, \mathcal{B}, \mathcal{E}^-) = \exp \left\{ -\frac{1}{2} \left[\sum_{i=1}^n (r_i^{(\mu_c)} - c_i \times g(\mathbf{x}_i; T, \mathcal{B}))^2 \right] \right\}. \quad (\text{A21})$$

introduce the partial residual

$$r_i^{(\mu_c)} = R_i^{(y)} + c_i \times g(\mathbf{x}_i; T, \mathcal{B}). \quad (\text{A22})$$

Then the conditional posterior density of the m -th tree is

Updating $\mathcal{E}^{(\tau)}$. To update the m -th tree $(T_m^{(\tau)}, \mathcal{B}_m^{(\tau)})$ in $\mathcal{E}^{(\tau)}$, we introduce the partial residual

$$r_i^{(\tau)} = R_i^{(y)} + c_i \times a_i \times g(\mathbf{x}_i; T, \mathcal{B}) \quad (\text{A23})$$

Then the conditional posterior density of the m -th tree is

$$p(\tilde{\mathbf{Y}}, \tilde{\mathbf{C}} | T, \mathcal{B}, \mathcal{E}^-) = \exp \left\{ -\frac{1}{2} \left[\sum_{i=1}^n (r_i^{(\tau)} - c_i \times a_i \times g(\mathbf{x}_i; T, \mathcal{B}))^2 \right] \right\}. \quad (\text{A24})$$

Updating $\mathcal{E}^{(n)}$. To update the m -th tree $(T_m^{(n)}, \mathcal{B}_m^{(n)})$ in $\mathcal{E}^{(n)}$, we set

$$p(\tilde{Y}, \tilde{C}|T, \mathcal{B}, \mathcal{E}^-) = \exp \left\{ -\frac{1}{2} \sum_{i=1}^n \left(r_i^{(n)} - g(\mathbf{x}; T, \mathcal{B}) \right)^2 \right\}, \quad (\text{A25})$$

where

$$r_i^{(n)} = R_i^{(c)} + g(\mathbf{x}_i; T, \mathcal{B}). \quad (\text{A26})$$

A.3 Updating splitting probabilities

Once we update each tree in \mathcal{E} , we update the elements of Θ conditionally on ξ and then update each element of ξ , conditionally on Θ . Update $\theta^{(\mu)}|\xi^{(\mu)}$ involves nothing more than a Dirichlet-Multinomial update. To update $\xi^{(\mu)}|\theta^{(\mu)}$, we use the Metropolis algorithm where proposals are drawn from the Beta(0.5, 1) prior on $\xi^{(\mu)}/(\xi^{(\mu)} + p)$. We similarly update the other components of Θ and ξ .

B Constant LATE Derivations

Reiterating Equation 3, the local average treatment effect, LATE is

$$\text{LATE} = \mathbb{E}[Y_i(1, 1) - Y_i(0, 0)|C_i = 1]. \quad (\text{B27})$$

This notation is made possible by Assumptions A1 and A2.

B.1 Observables

To show the identification of the estimators in the paper, we begin by formalizing the observed values. Potential outcome notation is made possible by Assumption A1.

$$R_i^{\text{obs}} = A_i R_i(1) + (1 - A_i) R_i(0) \quad (\text{B28})$$

$$Y_i^{\text{obs}} = A_i Y_i(1, R_i(1)) + (1 - A_i) Y_i(0, R_i(0)) \quad (\text{B29})$$

With the latter assumptions, these can be simplified to other useful quantities.

First, note that the definition of complier via Assumption A2 means $C_i = R_i(1)$, which confirms that complier-status is latent when $A_i = 0$. Combined with Assumption A2, where $R_i(0) = 0$, we see that

$$R_i^{\text{obs}} = A_i C_i + (1 - A_i)(0) = A_i C_i. \quad (\text{B30})$$

Second, we note that $Y_i(1, R_i(1)) = C_i Y_i(1, 1) + (1 - C_i) Y_i(1, 0)$, such that Assumptions A1 and A2 also lead to

$$Y_i^{\text{obs}} = A_i Y_i(1, R_i(1)) + (1 - A_i) Y_i(0, R_i(0)) \quad (\text{B31})$$

$$= A_i [C_i Y_i(1, 1) + (1 - C_i) Y_i(1, 0)] + (1 - A_i) Y_i(0, R_i(0)) \quad (\text{B32})$$

$$= A_i C_i Y_i(1, 1) + A_i (1 - C_i) Y_i(1, 0) + (1 - A_i) Y_i(0, 0) \quad (\text{B33})$$

and, as such, it is simple to show that the three summands above point to the three quantities we can most easily estimate with observables:

$$\mathbb{E}[Y_i^{\text{obs}}|A_i = 1, C_i = 1] = \mathbb{E}[Y_i(1, 1)|A_i = 1, C_i = 1] \quad (\text{B34})$$

$$\mathbb{E}[Y_i^{\text{obs}}|A_i = 1, C_i = 0] = \mathbb{E}[Y_i(1, 0)|A_i = 1, C_i = 0] \quad (\text{B35})$$

$$\mathbb{E}[Y_i^{\text{obs}}|A_i = 0] = \mathbb{E}[Y_i(0, 0)|A_i = 0]. \quad (\text{B36})$$

With these preliminaries, we expand these statements with the next two assumptions. Assumption A3 yields $Y_i(0, 0) = Y_i(1, 0)$, which changes Equation B33 to

$$Y_i^{\text{obs}} = A_i C_i Y_i(1, 1) + A_i(1 - C_i)Y_i(0, 0) + (1 - A_i)Y_i(0, 0) \quad (\text{B37})$$

$$= A_i C_i Y_i(1, 1) + (1 - A_i C_i)Y_i(0, 0). \quad (\text{B38})$$

Assumption A3 also augments Equation B35 into:

$$\mathbb{E}[Y_i^{\text{obs}}|A_i = 1, C_i = 0] = \mathbb{E}[Y_i(1, 0)|A_i = 1, C_i = 0] = \mathbb{E}[Y_i(0, 0)|A_i = 1, C_i = 0].$$

Assumption A4 means many of the above equations hold without being conditioned on assignment A_i :

$$\mathbb{E}[Y_i(1, 1)|C_i = 1] = \mathbb{E}[Y_i^{\text{obs}}|A_i = 1, C_i = 1] \quad (\text{B39})$$

$$\mathbb{E}[Y_i(1, 0)|C_i = 0] = \mathbb{E}[Y_i^{\text{obs}}|A_i = 1, C_i = 0] \quad (\text{B40})$$

$$\mathbb{E}[Y_i(0, 0)|C_i = 0] = \mathbb{E}[Y_i^{\text{obs}}|A_i = 1, C_i = 0] \quad (\text{B41})$$

$$\mathbb{E}[Y_i(0, 0)] = \mathbb{E}[Y_i^{\text{obs}}|A_i = 0]. \quad (\text{B42})$$

B.2 Identification of ITT_R

$$\begin{aligned} \mathbb{E}[R_i^{\text{obs}}|A_i = 1] - \mathbb{E}[R_i^{\text{obs}}|A_i = 0] &= \mathbb{E}[A_i R_i(1) + (1 - A_i)R_i(0)|A_i = 1] - \mathbb{E}[A_i R_i(1) + (1 - A_i)R_i(0)|A_i = 0] \\ &= \mathbb{E}[R_i(1)|A_i = 1] - \mathbb{E}[R_i(0)|A_i = 0] \\ &= \mathbb{E}[R_i(1)] - \mathbb{E}[R_i(0)] \\ &= \text{ITT}_R \end{aligned}$$

B.3 Identification of ITT_Y

$$\begin{aligned} \mathbb{E}[Y_i^{\text{obs}}|A_i = 1] - \mathbb{E}[Y_i^{\text{obs}}|A_i = 0] &= \mathbb{E}[A_i Y_i(1, R_i(1)) + (1 - A_i)Y_i(0, R_i(0))|A_i = 1] \\ &\quad - \mathbb{E}[A_i Y_i(1, R_i(1)) + (1 - A_i)Y_i(0, R_i(0))|A_i = 0] \\ &= \mathbb{E}[Y_i(1, R_i(1))|A_i = 1] - \mathbb{E}[A_i Y_i(1, R_i(1)) + (1 - A_i)Y_i(0, R_i(0))|A_i = 0] \\ &= \mathbb{E}[Y_i(1, R_i(1))] - \mathbb{E}[Y_i(0, R_i(0))] \\ &= \text{ITT}_Y \end{aligned}$$

B.4 The Wald Estimator

The standard estimator for the local average treatment effect for a binary instrument A_i is the Wald estimator (Wald, 1940), which is a ratio of the ITT_Y to ITT_R (Imbens and Rubin, 2015).

$$\frac{\text{ITT}_Y}{\text{ITT}_R} = \frac{\mathbb{E}[Y_i^{\text{obs}}|A_i = 1] - \mathbb{E}[Y_i^{\text{obs}}|A_i = 0]}{\mathbb{E}[R_i^{\text{obs}}|A_i = 1] - \mathbb{E}[R_i^{\text{obs}}|A_i = 0]} \quad (\text{B43})$$

which we can show is equivalent to LATE using the previously Assumptions A1-A5. First note the following simplifications of the expectations in the denominator.

$$\mathbb{E}[R_i^{\text{obs}}|A_i = 0] = \mathbb{E}[A_i C_i|A_i = 0] = 0 \quad (\text{B44})$$

$$\mathbb{E}[R_i^{\text{obs}}|A_i = 1] = \mathbb{E}[A_i C_i|A_i = 1] = \mathbb{E}[C_i|A_i = 1] = \mathbb{E}[C_i] = \mathbb{P}(C_i = 1) = \pi_C \quad (\text{B45})$$

where the second line uses the fact that $C_i = R_i(1)$ and Assumption A4, i.e. $A_i \perp R_i(1)$, which together yield $A_i \perp C_i$. Thus, the compliance rate $\pi_C = \mathbb{P}(C_i = 1)$ is something we can identify.

Now for the numerator of Equation B43, we already have part of it from Equation B42, so the remaining component identifies the following:

$$\begin{aligned}
\mathbb{E}(Y_i^{\text{obs}}|A_i = 1) &= \mathbb{E}[A_i C_i Y_i(1, 1) + (1 - A_i C_i) Y_i(0, 0)|A_i = 1] \\
&= \mathbb{E}[C_i Y_i(1, 1) + (1 - C_i) Y_i(0, 0)|A_i = 1] \\
&= \mathbb{E}[C_i Y_i(1, 1) + (1 - C_i) Y_i(0, 0)] \\
&= \mathbb{P}(C_i = 0) \mathbb{E}[C_i Y_i(1, 1) + (1 - C_i) Y_i(0, 0)|C_i = 0] + \mathbb{P}(C_i = 1) \mathbb{E}[C_i Y_i(1, 1) + (1 - C_i) Y_i(0, 0)|C_i = 1] \\
&= \mathbb{P}(C_i = 0) \mathbb{E}[Y_i(0, 0)|C_i = 0] + \mathbb{P}(C_i = 1) \mathbb{E}[Y_i(1, 1)|C_i = 1] \\
&= (1 - \pi_C) \mathbb{E}[Y_i(0, 0)|C_i = 0] + \pi_C \mathbb{E}[Y_i(1, 1)|C_i = 1]
\end{aligned}$$

Now, put it all together:

$$\begin{aligned}
\frac{ITT_Y}{ITT_R} &= \frac{\mathbb{E}[Y_i^{\text{obs}}|A_i = 1] - \mathbb{E}[Y_i^{\text{obs}}|A_i = 0]}{\mathbb{E}[R_i^{\text{obs}}|A_i = 1] - \mathbb{E}[R_i^{\text{obs}}|A_i = 0]} \\
&= \frac{(1 - \pi_C) \mathbb{E}[Y_i(0, 0)|C_i = 0] + \pi_C \mathbb{E}[Y_i(1, 1)|C_i = 1] - \mathbb{E}[Y_i(0, 0)]}{\pi_C - 0} \\
&= \frac{(1 - \pi_C) \mathbb{E}[Y_i(0, 0)|C_i = 0] + \pi_C \mathbb{E}[Y_i(1, 1)|C_i = 1] - (1 - \pi_C) \mathbb{E}[Y_i(0, 0)|C_i = 0] - \pi_C \mathbb{E}[Y_i(0, 0)|C_i = 1]}{\pi_C} \\
&= \frac{\pi_C \mathbb{E}[Y_i(1, 1)|C_i = 1] - \pi_C \mathbb{E}[Y_i(0, 0)|C_i = 1]}{\pi_C} \\
&= \mathbb{E}[Y_i(1, 1)|C_i = 1] - \mathbb{E}[Y_i(0, 0)|C_i = 1] \\
&= \text{LATE}.
\end{aligned}$$

C Tables: Simulations with multiple covariates

p	BCF-LATE				GRF				Ratio: GRF/BCF-LATE	
	RMSE	Coverage	Width	IS	RMSE	Coverage	Width	IS	RMSE	IS
2	0.115	0.883	0.352	0.018	0.797	0.955	2.503	0.066	6.965	3.765
5	0.110	0.901	0.356	0.017	0.455	0.955	1.678	0.045	4.181	2.714
10	0.108	0.910	0.367	0.016	0.355	0.966	1.665	0.043	3.326	2.706
25	0.103	0.924	0.385	0.016	0.273	0.977	1.469	0.038	2.673	2.392
50	0.101	0.931	0.405	0.016	0.164	0.933	0.897	0.026	1.629	1.634
75	0.102	0.930	0.404	0.016	0.177	0.836	0.727	0.027	1.740	1.701
100	0.116	0.926	0.452	0.017	0.213	0.730	0.704	0.035	1.915	2.086

Table C3: LATE(x) estimation performance for BCF-LATE and GRF on simple DGP. Metrics are averages for the 100 simulations, with n=2000. Coverage is 95% interval coverage, and ideally is 0.95. IS is the interval score of [Gneiting and Raftery \(2007\)](#), where smaller scores indicate better interval prediction. Ratios use BCF-LATE as a baseline, such that values greater than one indicate BCF-LATE performed better than GRF on average.

n	BCF-LATE				GRF				Ratio: GRF/BCF-LATE	
	RMSE	Coverage	Width	IS	RMSE	Coverage	Width	IS	RMSE	IS
500	0.210	0.730	0.447	0.037	0.337	0.886	1.535	0.048	1.616	1.332
2000	0.103	0.924	0.385	0.016	0.273	0.977	1.469	0.038	2.673	2.392
5000	0.069	0.965	0.326	0.011	0.350	0.989	1.752	0.044	5.076	4.161

Table C4: LATE(x) estimation performance for BCF-LATE and GRF on a simple data-generating process. Metrics are averages for the 100 simulations, with $p = 25$. Coverage is 95% interval coverage, and ideally is 0.95. IS is the interval score of [Gneiting and Raftery \(2007\)](#), where smaller scores indicate better interval prediction. Ratios use BCF-LATE as a baseline, such that values greater than one indicate BCF-LATE performed better than GRF on average.

p	BCF-LATE				GRF				Ratio: GRF/BCF-LATE	
	RMSE	Coverage	Width	IS	RMSE	Coverage	Width	IS	RMSE	IS
5	0.084	0.922	0.294	0.010	0.116	0.875	0.418	0.018	1.405	1.833
10	0.087	0.919	0.305	0.010	0.114	0.935	0.554	0.017	1.332	1.739
25	0.091	0.920	0.321	0.011	0.112	0.943	0.594	0.018	1.241	1.754
50	0.093	0.921	0.329	0.011	0.111	0.939	0.579	0.018	1.207	1.707
75	0.094	0.921	0.333	0.011	0.111	0.945	0.611	0.019	1.199	1.728
100	0.094	0.929	0.339	0.011	0.114	0.949	0.650	0.019	1.230	1.791

Table C5: LATE(x) estimation performance for BCF-LATE and GRF on a challenging data-generating process. Metrics are averages for 100 simulations, with $n=2000$ and only five covariates involved in the DGP. Coverage is 95% interval coverage, and ideally is 0.95. IS is the interval score of [Gneiting and Raftery \(2007\)](#), where smaller scores indicate better interval prediction. Ratios use BCF-LATE as a baseline, such that values greater than one indicate BCF-LATE performed better than GRF on average.

n	BCF-LATE				GRF				Ratio: GRF/BCF-LATE	
	RMSE	Coverage	Width	IS	RMSE	Coverage	Width	IS	RMSE	IS
500	0.106	0.922	0.395	0.013	0.135	0.946	0.707	0.021	1.289	1.640
2000	0.091	0.920	0.321	0.011	0.112	0.943	0.594	0.018	1.241	1.754
5000	0.074	0.932	0.267	0.009	0.101	0.953	0.572	0.017	1.385	2.024

Table C6: LATE(x) estimation performance for BCF-LATE and GRF on a challenging data-generating process. Metrics are averages for the 100 simulations, with $p = 25$ but only five covariates involved in the DGP. Coverage is 95% interval coverage, and ideally is 0.95. IS is the interval score of [Gneiting and Raftery \(2007\)](#), where smaller scores indicate better interval prediction. Ratios use BCF-LATE as a baseline, such that values greater than one indicate BCF-LATE performed better than GRF on average.